HETEROGENEOUS SURFACE-BASED FREEZING OF ATMOSPHERIC AEROSOLS CONTAINING ASH, SOOT, AND SOIL

A Thesis

by

ADAM PATRICK FORNEA

Submitted to the Office of Graduate Studies of
Texas A&M University
in partial fulfillment of the requirements for the degree of

MASTER OF SCIENCE

May 2009

Major Subject: Atmospheric Sciences

HETEROGENEOUS SURFACE-BASED FREEZING OF ATMOSPHERIC AEROSOLS CONTAINING ASH, SOOT, AND SOIL

A Thesis

by

ADAM PATRICK FORNEA

Submitted to the Office of Graduate Studies of
Texas A&M University
in partial fulfillment of the requirements for the degree of

MASTER OF SCIENCE

Approved by:

Chair of Committee,	Sarah D. Brooks
Committee Members,	Ping Yang
	Brent V. Miller
Head of Department,	Kenneth P. Bowman

May 2009

Major Subject: Atmospheric Sciences

ABSTRACT

Heterogeneous Surface-Based Freezing of Atmospheric Aerosols Containing Ash, Soot, and Soil. (May 2009)

Adam Patrick Fornea, B.S., Texas A&M University

Chair of Advisory Committee: Dr. Sarah Brooks

Nucleation of ice crystals in the atmosphere often occurs through heterogeneous freezing processes facilitated by an atmospheric aerosol that acts as the ice nuclei (IN). Depending on ambient conditions and aerosol composition, heterogeneous nucleation will occur through one of several mechanisms including the contact and immersion freezing mechanisms. Through a series of contact freezing experiments, we have characterized the ability of aerosols composed of volcanic ash, soot, and peat soil, to act as ice nuclei (IN) as a function of temperature. The immersion freezing ability of the ash particles has also been measured. In these studies, an optical microscope apparatus equipped with a cooling stage and a digital camera was used to observe the freezing events. For each experiment, a particular IN was placed in contact with the surface, or immersed in the bulk, of an ultra pure water droplet. The droplet was then subjected to freezing-melting cycles resulting in 25 independent measurements of the freezing temperature of the droplet. In the volcanic ash experiments, we observed contact freezing at warmer temperatures than immersion freezing. As contact freezing IN, the peat was the most effective with an average contact freezing temperature of -10.5 °C, followed by volcanic ash (-11.2 °C), and then soot (-25.6 °C). In addition, we have used classical

nucleation theory to identify the contact parameters and nucleation rates for the compositions explored.

ACKNOWLEDGEMENTS

I would like to thank my committee chair, Dr. Sarah Brooks, and my committee members, Dr. Ping Yang, and Dr. Brent Miller, for their guidance and support throughout the course of this research.

I would like to thank Dr. Brent Miller and Dr. Franco Marcantonio of the Geology Department at Texas A&M University, and Zamin Kanji from the University of Toronto for insightful discussions. I thank Brandon Dooley, from the Texas A&M Engineering Department, for his thoughtful discussions, ideas, assistance, and work in this study. I must also thank the National Science Foundation (NSF) for providing the funding for this study.

Thanks also go to all of my friends in the Atmospheric Sciences department at Texas A&M University, including all faculty and staff members, for making my academic career a fun and meaningful experience. I thank my friends and family, especially my wife Ericka, for supporting me always through all of life's ups and downs. I would also like to thank my mother and father, without whom none of my success would be possible, and I give them a great deal of credit for keeping me going and being amazing parents.

I also thank God for allowing me this chance to contribute to the scientific understanding of this wonderful world He has given us. Stephen Hawking once said, "My expectations were reduced to zero when I was 21. Everything since then has been a bonus." I have received my bonus as well, and I intend to make the most of the time I have left.

TABLE OF CONTENTS

LIST OF FIGURES

LIST OF TABLES

1. INTRODUCTION

Formation of ice particles in the absence of ice nuclei, which is termed homogeneous freezing, can only occur at very low atmospheric temperatures. Based on experimental data and estimates of theoretical parameters for the homogeneous freezing of a pure water droplet, cloud droplets of sizes relevant to the atmosphere are expected to freeze spontaneously at or below ~ -40 ^{o}C (Rogers and Yau, 1989; Wallace and Hobbs, 2006). Since pure water is uncommon in the atmosphere, crystals of pure ice rarely form. Instead, ice particle formation occurs through either homogeneous freezing of a solution droplet or by one of a variety of heterogeneous mechanisms (Rogers and Yau, 1989). In recent years, a large number of experiments on the homogeneous freezing mechanism of sulfate aerosols have greatly advanced our understanding of the processes of homogeneous freezing (Bertram, 1996; Koop, 1998, 2000; Chang et al., 1999; Chelf and Martin, 1999; Chen et al., 1999; Cziczo, 1999; Krämer et al., 1999; Onasch et al., 1999; Yao et al., 1999; DeMott, 2000; Prenni et al., 2001). However, our understanding of ice nucleation at warmer temperatures and lower relative humidities is still much more limited. Under these conditions in the atmosphere, any nucleation that occurs is heterogeneous and is facilitated by an atmospheric particle, referred to as an ice nucleus (IN). Since these IN make nucleation possible under a much broader range of conditions than over which homogeneous freezing can occur, even relatively small populations of IN ($\geq$ 1 liter^{-1}) can have substantial impacts on the overall development of an ice cloud (DeMott et al., 1994; Rangno and Hobbs, 1990; 1994).

This thesis follows the style of *Journal of Geophysical Research*.

The release of aerosols into the upper troposphere may increase the efficiency of cirrus cloud formation via heterogeneous ice nucleation, and thereby possibly cause significant alterations in Earth's radiative budget (IPCC, 2007). Cirrus cloud cover has recently been shown to be as high as 40% in the tropics (Wylie et al., 1994), and these clouds have been shown to primarily consist of small ice particles with diameters smaller than 50 μm (Yang et al, 2003). Such ice crystals are highly effective at scattering sunlight and thus have a large effect on Earth's radiative energy budget (Garrett et al., 2003). There are four basic pathways of heterogeneous ice nucleation in the atmosphere: condensation freezing, immersion freezing, contact freezing, and deposition nucleation (Pruppacher and Klett, 1997; Vali, 1985). For the purposes of this study, we are only concerned with immersion and contact freezing.

Research on atmospheric ice nucleation has advanced quite far recently, but conducting studies in this field remains a challenging task. Most field and laboratory methods for measuring heterogeneous ice nucleation are efficient for determining the conditions required for nucleation to occur and total concentrations of nucleating crystals, but lack the ability to distinguish between heterogeneous mechanisms (Pruppacher and Klett, 1997). For example, a Continuous Flow Diffusion Chamber (CFDC) is capable of measuring nucleation activity under conditions in which deposition and condensation freezing may prevail, yet all ice crystals are grouped together and total IN concentration is reported, indiscriminate of mechanism (Rogers, 1988). In another method, Fourier Transform Infrared Spectroscopy (FTIR) is used to observe the freezing of an ensemble of aerosols in a double-walled flow tube apparatus at selected temperatures and relative

humidities (Bertram et al., 1996; Onasch et al., 1999). As in other studies, it can only be postulated which heterogeneous ice mechanism prevailed.

However, a limited amount of mechanism-specific heterogeneous ice nucleation studies have been carried out. Most of these examine deposition nucleation, as it remains the mechanism that is most effectively simulated in the laboratory. Some of these studies have indicated that deposition nucleation is an efficient mode of heterogeneous ice nucleation for specific mineral dusts present in the atmosphere, but that it is not an efficient pathway of nucleation for some combustion particles such as n-hexane soot (Kanji and Abbatt, 2006, 2008). Several experiments have been done that characterize contact or immersion freezing. In one such experiment, exhaust particles from a kerosene burner are tested for ice nucleating ability by each of the four heterogeneous mechanisms (Diehl and Mitra, 1998). In their experimental setup that characterizes contact freezing, pure water droplets that are suspended in a wind tunnel and held at consistently low temperatures. The droplets are then exposed to a moving flow of kerosene-burner exhaust particles, and if the contact between the droplet and the particles causes freezing, it is recorded as a contact freezing event at that temperature. Several other studies have examined the contact and immersion freezing temperatures of droplets using a cooling apparatus combined with a microscope (Durant and Shaw, 2005; Shaw et al. 2005).

It has been shown by many investigations that within a single mechanism of heterogeneous ice nucleation, there exists much variability in freezing temperatures due to differences in the intrinsic properties of the IN (Levin and Yankofsky, 1964; Vali 1968; Schnell, 1972, 1974; Diehl et al. 1998, 2002; von Blohn et al., 2005). While it is

not certain which specific aerosol properties are most important in determining the overall IN effectiveness of an aerosol, it is known that solubility and hydrophobicity contribute to how well a particle can assist in contact ice nucleation (Pruppacher and Klett, 1997). Insoluble particles are often effective IN as they provide solid substrates on which ice formation can begin. However, if a particle is very hydrophobic it will minimize its contact with a water droplet, thereby decreasing the total amount of surface area and favorable IN sites available to facilitate nucleation. Since solubility and hydrophobicity depend on composition, composition and source of IN are very important in ice nucleation studies. Aerosol size is also important in determining the aerosol's effectiveness as an IN (Jaenicke, 1993). The effects of particle size and composition are interconnected, since aerosols of certain compositions are typically found in certain size ranges. The most effective IN are often large in volume and surface area, insoluble, and also do not possess hydrophobic tendencies.

One type of particle in the atmosphere that can possess these qualities is ash from volcanic eruptions. The eruption of Mount St. Helens in May of 1980 was one of the largest in North American recorded history, and it released over one billion cubic meters of volcanic ash into the air (Brantley and Myers, 2000). A chemical analysis by Fruchter et al. (1980) revealed that the ash produced by the 1980 Mt. St. Helen's eruption was dacitic in composition and had a silica concentration of approximately 65%. Volcanic ash particles in the atmosphere have been shown to be effective IN in many studies (e.g. Mason and Maybank, 1958; Isono et al, 1959; Isono and Ikebe, 1960; Schnell et al, 1982). However, Price and Pales (1963) have shown volcanic ash particles from eruptions on the Hawaiian Islands not to possess such a high efficiency as IN. The reasons for the

differences in these results are not well understood, but differences in chemical composition based on large distances between the geographical locations of the respective volcanic activity are likely responsible.

Humic-like substances (HULIS) are important primary aerosol constituents with sources such as soil, vegetation, and biomass burning (Dinar et al, 2006 and references contained therein). HULIS also can be formed within the atmosphere as a result of the photo-oxidation of primary biogenic and anthropogenic precursors. HULIS are composed of a mixture of organic structures such as aromatic, phenolic, and acidic functional groups. Particles containing humic substances are of great importance to atmospheric scientists because of their presence in many different types of surface soils, and also because they resemble HULIS in their high molecular weight and chemical structure (Graber and Rudich, 2006). To the best of our knowledge, there are no measurements to date of heterogeneous freezing for humic acid particles.

Upon emission, soot is an insoluble and extremely hydrophobic substance. Compared to many other atmospheric aerosols it is relatively inefficient as an IN without some form of chemical aging or the addition of a coating (Demott, 1990; Wyslouzil et al., 1994; Gorbunov et al., 2001; Dymarska et al. 2006). Once soot particles undergo atmospheric oxidation processes, they have been shown to be active as cloud condensation nuclei (CCN) as well as IN (Pöschl, 2005; Dymarska et al. 2006). One explanation for this is that during the aging process, oxygenated functional groups may be added to the surface of the organic aerosol, causing an increase in the polarity of the particle surface and reduced hydrophobicity (Sun and Ariya, 2004). Soot particles can also become more hydrophilic by acquiring a coating of a water-soluble substance such

as sulfuric or nitric acid via deposition in the atmosphere (Wyslouzil 1994; Chughtai et al., 1996).

For our experimental IN, we chose Mount St. Helens volcanic ash that was collected after the eruption in May of 1980, Pahokee Peat Soil II obtained from the International Humic Substances Society (IHSS), and carbon (Lampblack) obtained from the Fisher chemical company.

1.1 Contact Freezing Mechanisms

Traditionally, immersion freezing is defined as "Nucleation of supercooled water by a nucleus suspended in the body of water," and contact freezing is defined as "Nucleation of a supercooled droplet subsequent to an aerosol particle's coming into contact with it," (Vali, 1985). The standard immersion freezing definition aptly describes the immersion measurements included in this study. However, recent findings suggest that traditional contact freezing, which we will refer to as collisional contact freezing, could be just one pathway of a broader surface-based mechanism (Shaw et al., 2005; Durant and Shaw 2005).

Shaw et al. (2005) and Durant and Shaw (2005) conducted experiments where an IN is placed in contact with the water-air interface of a droplet, from either the inside or the outside of the droplet, at the beginning of their setup. Freezing events are then observed as the droplet temperature is reduced at a constant rate. The authors call this mode of freezing "contact freezing inside-out" to distinguish it from contact freezing involving a collision. Collisional contact freezing, where an IN comes into contact with the surface of a water droplet, occurs at roughly 10-15 K higher than does the

homogeneous freezing of pure water, and also 2-5 K higher than the mechanism of immersion freezing for most IN compositions studied (Gokhale and Goold, 1968; Pitter and Pruppacher, 1973; Fukuta, 1975; Diehl et al., 2002). The results in Shaw et al. (2005) and Durant and Shaw (2005) show a "very similar" increase in ice nucleation efficiency for contact freezing inside-out relative to immersion freezing. Their results also show that the contact freezing temperatures are identical whether the IN is placed at the outside or inside of the droplet surface (Durant and Shaw, 2005). These are informative results since in early studies contact freezing was thought to occur via collision between completely dry particle and a supercooled droplet (Fletcher, 1969, Cooper 1974). Prior to collision, the dry IN theoretically has a tiny 'ice embryo' on its surface deposited from the vapor phase. Once the ice embryo contacts the droplet, it acts as a template, initiating the freezing of the entire droplet. Shaw's results indicate that the particle need not be dry to act as an effective IN, but does need to contact the droplet surface. This opens up additional atmospheric applications of the contact freezing mechanism. For instance, if a droplet containing an IN undergoes evaporation of outer layers of water and leaves the IN at the surface, ice nucleation may occur. In this study, we extend the work of Shaw et al. (2005) and Durant and Shaw (2005) by conducting similar contact freezing experiments on a range of atmospherically relevant compounds.

Much of the current work on heterogeneous ice nucleation theory involves attempting to understand how the beginnings of a freezing event, termed ice embryos, overcome a free energy barrier to reach a critical size. As mentioned previously, it was suggested that collisional contact freezing occurred when sub-critical ice embryos formed via water vapor deposition on the surface of an IN were submerged into a water droplet

during a collision (Cooper, 1974). The critical size for ice embryos formed through deposition is much larger than for immersion. Once these embryos were submerged, they were no longer of sub-critical size and they caused a freezing event. However, it has been argued that these embryos would undergo rapid changes in both radius and contact angle as the IN surface is flooded upon collision, which would not permit freezing to occur from those embryos (Fukuta, 1975). In addition, this mechanism provides no explanation for the difference in efficiencies between contact and immersion freezing.

Fukuta (1975) argued that there was simply an increase in free energy, and subsequently a reduction in the free energy barrier required for freezing, caused by the moving water-IN boundary as a colliding IN goes into a water droplet. Thus, he argued, it is the mechanical contact event between an IN and a water droplet that is responsible for producing a freezing event. However, this mechanism has received criticism for not explicitly relating the free energy increase produced by the differences in interfacial energies and the free energy needed to form a supercritical ice embryo (Young, 1993).

Since contact freezing inside-out involves no collision, none of these previously proposed mechanistic explanations would provide an understanding for how these freezing events would occur. Shaw et al. (2005) argue that the increase in nucleation efficiency seen between immersion freezing and freezing with an IN in constant contact with the water-air interface is a result of the free energy barrier for ice nucleation being lower at the surface of a droplet than it is in the bulk, which is in accordance with the arguments of Djikaev et al. (2002). The authors further argue that collisional contact freezing is quite possibly a manifestation of this increased nucleation efficiency caused by the same mechanism (Durant and Shaw, 2005).

While there is a growing body of literature on heterogeneous ice nucleation processes, measurements involving either collisional contact freezing or contact freezing inside-out are much more limited. The studies that explicitly concern such surface-based freezing (Gokhale and Goold, 1968; Gokhale and Lewinter, 1971; Gokhale and Spengler, 1971; Sax and Goldsmith, 1971; Pitter and Pruppacher, 1973; Young, 1974; Rosinski and Nagamoto, 1975; DeMott et al., 1983; Levin and Yankofsky, 1983; Deshler and Vali, 1991; DeMott, 1994; Diehl and Mitra, 1998; Diehl et al., 2002; Finnegan, 1998; Lohmann, 2001; DeMott et al., 2005; Shaw et al., 2005; Durant and Shaw, 2005) use a variety of techniques and particle compositions in an attempt to further characterize a heterogeneous atmospheric pathway that remains quite difficult to simulate in controlled experiments. Still, a number of papers on field measurements (Young, 1974; Cooper and Vali, 1981; DeMott et al., 1983; Hobbs and Rangno, 1985; Cooper, 1986; Rangno and Hobbs, 1991; Beard, 1992; Rangno and Hobbs, 1994; Cooper 1995; Field et al., 2001; Cotton and Field, 2002; Ansmann et al., 2005; Baker and Lawson, 2005; Lawson et al., 2006) suggest that while surface-based freezing is virtually unexplored, it is an important mechanism in the atmosphere. These studies suggest that much of the ice formed in the lower troposphere may be due not only to the straightforward manifestations of surface-based freezing, but also may be a result of evaporative freezing through contact freezing inside-out. In particular, Beard (1992) points out that although evaporative freezing has been thought to be an efficient process, the reasons for its efficiency have never been fully explained. Durant and Shaw (2005) provide a possible explanation for this in that a droplet with an IN inside of it would freeze at a higher rate as the droplet evaporated to provide contact with the IN particle.

It is noteworthy that surface-initiated crystallization has also been a recent focus of several important homogeneous ice nucleation studies (Djikaev et al., 2002; Tabazadeh et al., 2002; Djikaev et al., 2003; Kay et al., 2003; Duft and Leisner, 2004; Sigurbjörnsson and Signorell, 2008). In a reanalysis of laboratory data collected in several laboratories using a range of measurement techniques, Djikaev et al. (2002 and 2003) and Tabazadeh et al. (2002) have some shown that agreement among derived nucleation rates is much better when surface-based, rather than a volume based rates are compared. However, these studies have come under scrutiny by later works that show that combined uncertainties in both the thermodynamic assumptions made, and at least some of the current experimental techniques for analysis, make definitively distinguishing between surface and volume mechanisms unlikely (Kay et al., 2003; Duft and Leisner, 2004; Sigurbjörnsson and Signorell, 2008). While efforts to refine the surface-based theory are ongoing, more measurements strategically designed to address the issue of surface versus volume are needed to fully understand the role of surface initiation in both homogeneous and heterogeneous freezing.

In this study, we attempt to extend the arguments of Shaw et al. (2005) and Durant and Shaw (2005) by using a similar methodology to show the difference in nucleation efficiency between contact and immersion freezing using Mount St. Helens volcanic ash as IN. Further, we explore the contact freezing efficiency of both IHSS Pahokee Peat Soil II and carbon (lampblack).

2. EXPERIMENTAL METHODS

In these experiments, an ultra pure water droplet (HPLC grade) is observed as its temperature is reduced at a controlled rate (1.0 ^{o}C min^{-1}) to assess how a certain IN affects the freezing temperature of the droplet via contact or immersion freezing. A droplet containing a single IN is frozen, melted, and refrozen many times during one experiment. The freezing temperatures for the droplet on each cycle are derived using digital imaging devices and temperature measurements. We gather numerous data points with the same setup, which limits the number of possible variables in the experiment (Durant and Shaw, 2005; Shaw et al., 2005). This method is advantageous because ice nucleation is theorized to primarily be a stochastic process, and therefore getting multiple data points on the same IN is desirable.

In our experimental setup, using a tank of dry nitrogen gas and a Nalgene bubbler, a low flow of humidified nitrogen gas is generated and passes through the cooling stage during experiments. This flow prevents the droplet from evaporating. This flow setup, as shown in Figure 1, consists of dry and humidified flows separately controlled by mass flow controllers (Model MC-10SLPM-D(N2), Alicat) and then mixed together before entering the cold stage. Specifically, a humidified nitrogen flow of 0.03 L min^{-1} and a dry nitrogen flow of 0.57 L min^{-1}, which produce a total flow through the chamber of 0.60 L min^{-1}, are used in all experiments unless otherwise noted. The dewpoint is measured and monitored using a dewpoint hygrometer (Model 2000 series DewPrime II, EdgeTech). These flow settings were optimal because they gave the air enough humidity at the warmer temperatures to prevent the evaporation of our droplet during

experiments. This additional humidity added to the experiment did not produce any detectable condensational growth of our droplets, nor did it produce condensation of water or deposition of ice on the IN when placed outside the droplet.

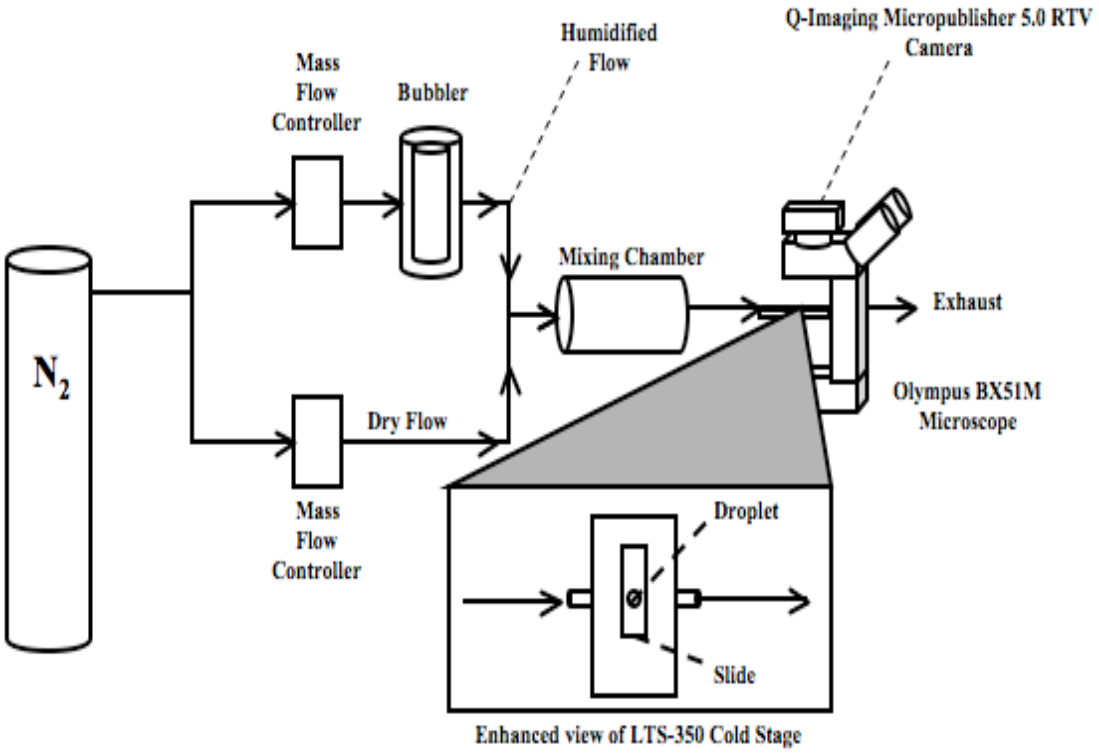

Figure 1: Our experimental setup is shown.

The cold stage (Model LTS-350, Linkam) is a sealed chamber that allows for the temperature control of the surface on which samples sit to a sensitivity of a tenth of a degree. The stage is connected to both a temperature controller box and a liquid nitrogen pump, which are both controlled by software (Model Linksys 32-DV, Linkam). This system acts to adjust the flow of liquid nitrogen pumped into the stage during cooling,

and controls the heating between freezing cycles. This allows us to run experiments within specific temperature boundaries at very precise temperature change rates. The cold stage sits upon an optical microscope (Model BX51M, Olympus) equipped with a digital camera (Model Micropublisher 5.0 RTV, Q-Imaging) that allows for visual monitoring of the freezing temperatures of the droplets. The images from the camera are sent to the Linksys 32 software and are captured at a rate of one image every six seconds, which is frequent enough to record a single image at every tenth of a degree.

Prior to each experiment, samples are prepared outside of the cold stage in a clean environment. The sample is then placed into the cold stage, and the stage is sealed. We produce the samples by placing an ultra pure water droplet (HPLC grade) of specific volume on a silanized microscope slide of approximately 0.8 mm thickness. The slides are silanized by immersing a plain glass microscope slide (VWR) in a 1.0% Aquasil solution (Pierce Chemical Company), and this produces a coating on the slide that is significantly hydrophobic. The hydrophobic surface prevents condensation on the microscope slide that, if present, could interfere with the accuracy of the experimental results. In addition, the coating minimizes the contact between the microscope slide and the water droplet, which not only reduces the possibility of the slide acting as a nucleation substrate for the droplet, but also allows the droplet to retain a more spherical shape as it would have in the atmosphere. The specific droplet size is attained by using an Eppendorf research micropipettor, which can be adjusted to produce droplets with a specific volume ranging from 0.1-2.5 μL. For this study the droplet volume is held constant at 2.0 μL.

Once the droplet is placed on the slide, a specific type of particle is selected to serve as an IN. Using 3" diameter testing sieves from Newark Wire Cloth Company, we have size-selected all IN to be in the size range of 250 μm to 300 μm for their diameter. Assuming a spherical shape of the IN, we can estimate that this provides between 0.78 and 1.1 mm^2 of total IN surface area on which nucleation can occur. Size-selection limits the effects that IN of various sizes could have upon the experiments, and allows us to monitor the effects of varying chemical composition more carefully. The IN is then carefully positioned using a hypodermic syringe either at the surface of the droplet or completely immersed in the bulk (middle) of the droplet depending on whether contact or immersion freezing is desired. Solely contact freezing is tested with the peat and soot IN by placing them on the outside of the water-air interface. We test both contact and immersion freezing with the volcanic ash IN by placing the IN either on the inside of the water-air interface or in the bulk of the droplet. There is previous evidence that contact freezing occurs at the same temperature regardless of whether the IN is in contact with a droplet's surface from the inside or the outside of a droplet (Durant and Shaw, 2005). Thus, we do not differentiate between experiments regarding inside or outside contact freezing. After the slide has a droplet with an IN in the desired position, it is placed in the slide holder within the stage, and the stage is sealed.

To ensure that the IN were in the desired position, and thus were either definitely in contact with the inside or outside of the droplet surface or definitely not in contact, we employed a simple optical methodology. By exploiting the distinct focal plane associated with compound light microscopes the position of the IN can be found with relative certainty. This technique utilized a boom-mounted compound microscope set in a

horizontal orientation. Such a configuration allowed the droplet to be viewed from the side, placing the focal plane perpendicular to the horizontal glass microscope slide on which the droplet resided. By adjusting the focus on the microscope, it was possible to calculate the difference in position between the center focal plane of the droplet and the IN particle as is shown in Figure 2. Since our droplet size is known and in a constant range, as is our IN size, we can definitively say whether the IN is in contact with the droplet's surface. This technique is described in further detail in Appendix A. Furthermore, this side view produces pictures (Figure 3) from an alternate angle that help us to be certain of the position of the IN.

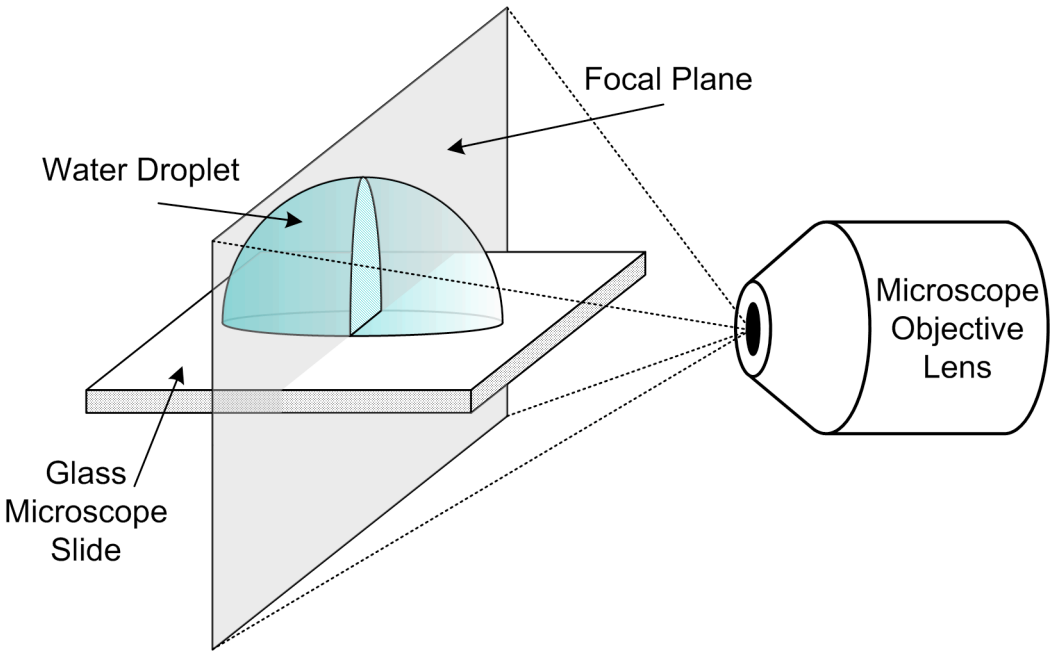

Figure 2: Our method for verifying the position of the IN within the droplet is illustrated here.

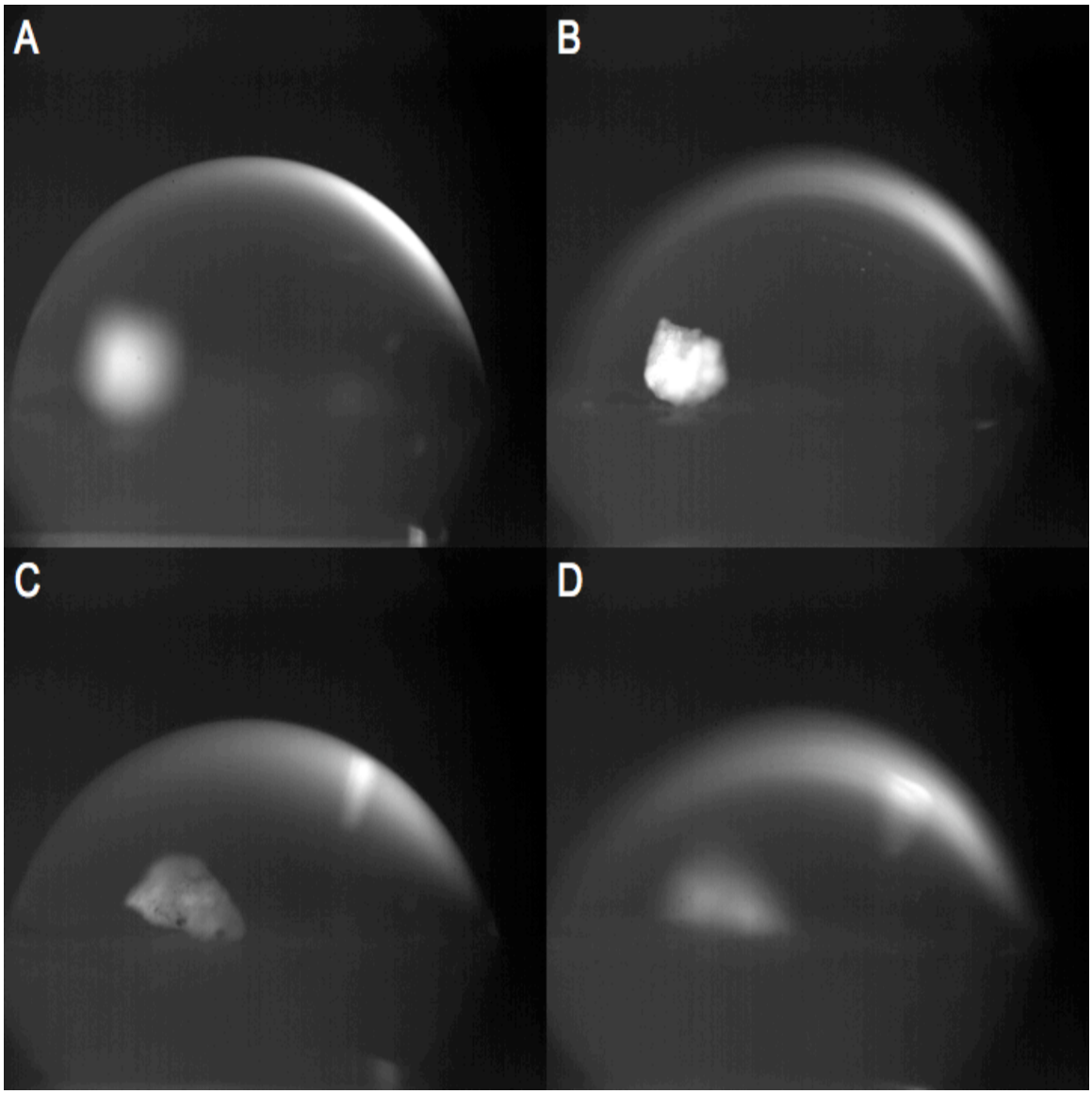

Figure 3: Side-view images that further depict our method for verifying the position of the IN. In panels A and B, the IN particle is located at the edge of the droplet closest to the camera, while the focal plane in panel A is at the center of the droplet and the focal plane in panel B is at the front edge of the droplet. In panels C and D, the IN particle is located in the bulk of the droplet, while the focal plane in panel C is at the center of the droplet and the focal plane in panel D is at the front edge of the droplet. The droplet and IN particle is the same for all panels despite some visible rotation of the IN that occurred while moving the particle from the edge to the middle.

Once the experiment is prepared, temperature control and data collection are handled by the Linkam equipment and the Linksys 32-DV software. The software is set

to cool the stage from its beginning temperature of 5.0 °C down to -40 °C at a rate of 1.0 °C per minute. Once -40 °C is reached, the software immediately begins warming the stage back up to 5.0 °C at the same rate. The software then remains at a temperature of 5.0 °C for one minute to ensure complete melting of the droplet, and then the cycle is repeated. The number of cycles that can be performed for each experimental setup is 25, limited only by the size of the liquid nitrogen dewar which supplies liquid nitrogen to the cooling stage.

We chose to use a cooling rate of 1.0 °C/min after a comparison between different cooling rates showed a significant offset between the temperature experienced on the slide by the water droplet and the stage's temperature sensor. In five cooling rate comparison experiments, when 10 °C/min was compared with 1.0 °C/min, there was an average offset between freezing temperatures of 3.6 °C/min. In three cooling rate experiments, when 5.0 °C/min was compared with 1.0 °C/min, there was an average offset between freezing temperatures of 1.4 °C. Finally, in three cooling rate comparison experiments, when 2.0 °C/min was compared with 1.0 °C/min, there was an average offset between freezing temperatures of 0.3 °C/min. This showed that the mean freezing temperatures for the rates of 2.0 °C/min and 1.0 °C/min were not statistically different at the 95% confidence level. These results are depicted in Figure 4. We used 1.0 °C/min as our cooling rate because it provided us with the most freezing points for our dewar capacity without sacrificing the integrity of our data.

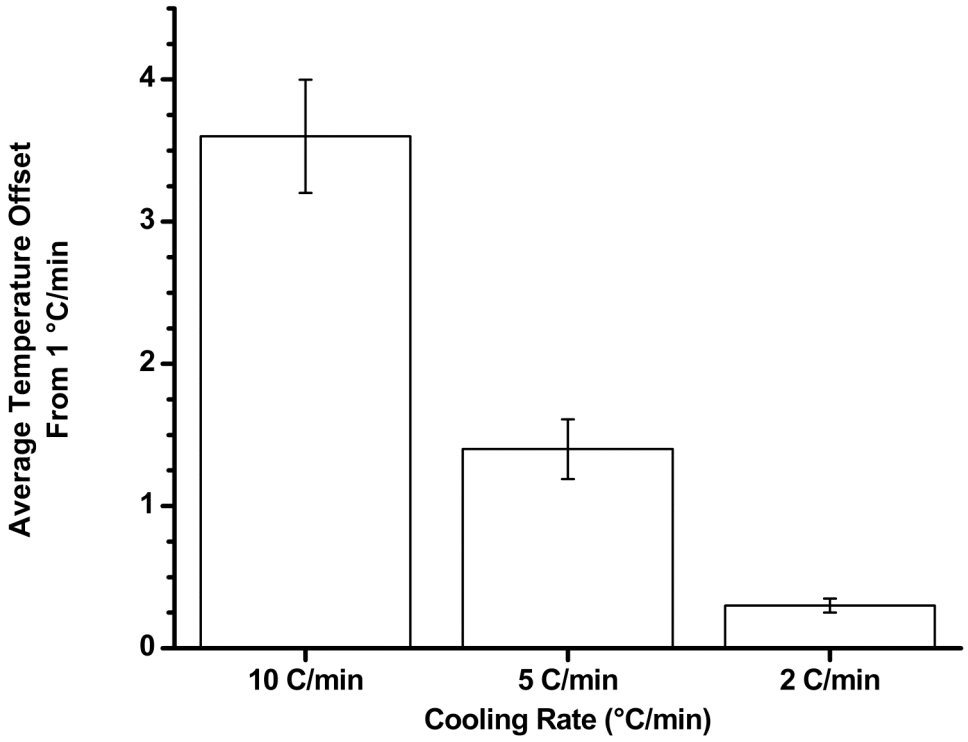

Figure 4: The average temperature offsets between 1 °C/min and other cooling rates are shown. The error bars shown are the total standard error for each average offset.

The Linksys software records a high-resolution image from a Micropublisher 5.0 RTV camera once every six seconds. These images are used in post-experimental analysis to determine the freezing point of the droplets as precisely as possible. For the purposes of this experiment, we define the freezing point as the temperature at which first visual evidence is received of the beginning of a freezing event for the droplet. The freezing event is characterized by a wave of motion through the droplet, followed by a very obvious change in opaqueness and reflectivity of the droplet with the eventual appearance of ice. Such a freezing event is shown in Figure 5.

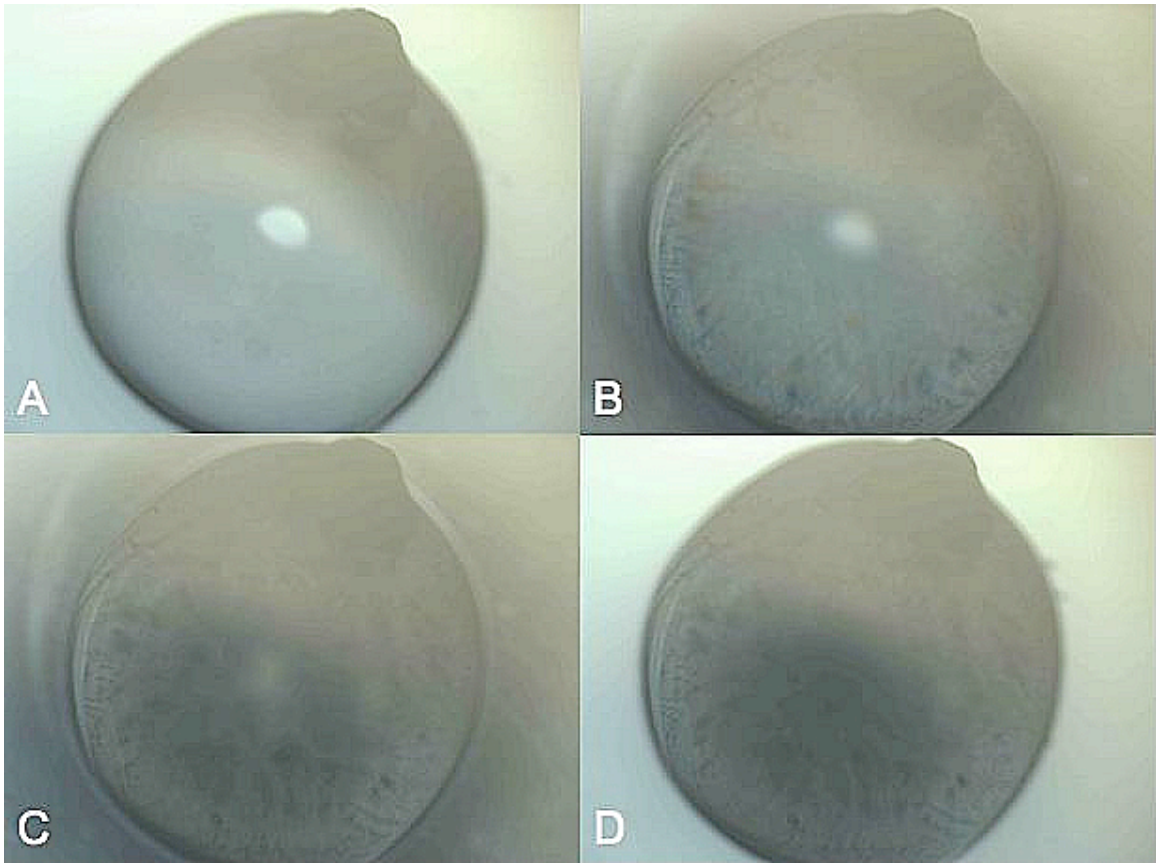

Figure 5: A freezing event during an experiment using a peat IN. The 4 pictures are shown in sequential order, with the panel A being the unfrozen droplet prior to freezing, panel B being the beginning of the freezing event, panel C being the continuation of solidification, and panel D being the resultant completely frozen droplet. Here we would classify panel B as our freezing point. The condensation seen in panels B and C is a result of the enthalpy of freezing, and quickly evaporates after the freezing event is over, as can be seen in panel D. Focus is on the droplet so as to attain the beginning of the freezing event as precisely as possible, but the peat IN can be seen on the upper right surface of the droplet.

By performing the aforementioned frame-by-frame post-experimental analysis of the digital images, it is possible to accurately and reproducibly identify the freezing temperatures of our droplets within the numerous cycles of a particular experiment. This is illustrated in Figure 7, which shows the first 10 cycles of an experiment using volcanic

ash as the IN. Some experiments produce much variability between freezing points, and yet some remain consistent within a few tenths of a degree all the way through the experiment. We occasionally observe IN movement during melting and freezing events, and also IN breakup in the case of experiments featuring peat particles, which were more fragile than the other IN. We attribute increasing variability within a single experiment to characteristics such as these, while variability from experiment to experiment may be due primarily to variations in the intrinsic properties of the IN.

a.)

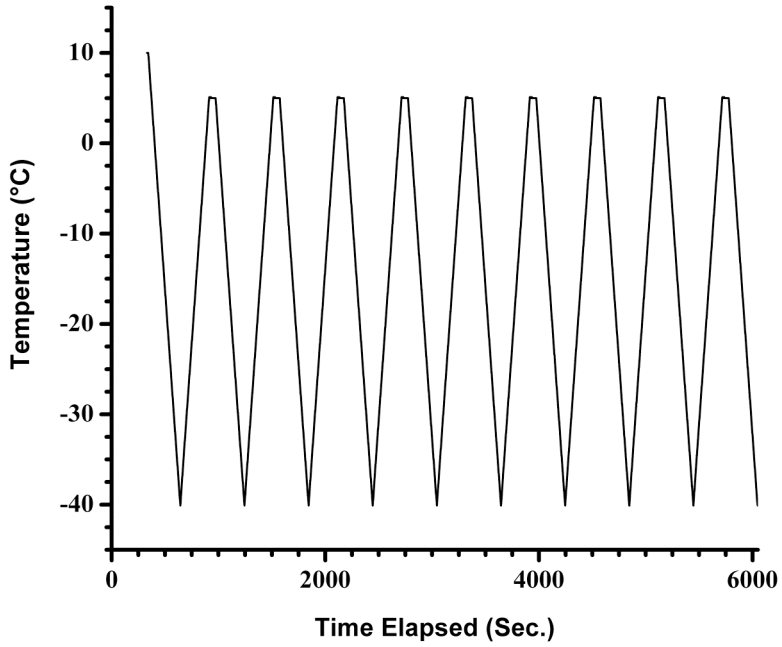

Figure 6: As an example, the first 10 cycles of a single setup, with volcanic ash as the IN and 2.0 μL as the droplet volume, are shown. In a.), the temperature of the stage is shown as it is being controlled by the Linksvs software.

b.)

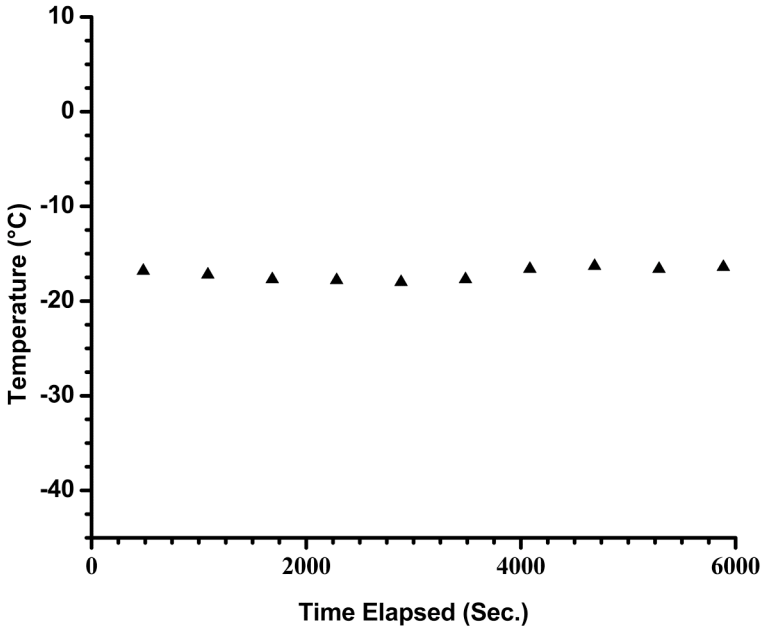

Figure 6 Continued. In b.), the individual freezing points are shown as acquired from post-experimental analysis of the images.

3. RESULTS

In this section, we report our results for the comparative study between contact and immersion freezing for volcanic ash, as well as the relative contact freezing efficiency of all three of our chosen IN types. First, to assess the amount of uncertainty involved in the recorded temperature data, we performed a calibration of the stage by running experiments using pure water droplets without a contacting IN. We also ran some experiments to test the well-documented melting point of mercury.

3.1 Characterization of Cooling Stage Temperatures

As additional confirmation of our measured temperatures, we performed experiments on a specific compound with a well-documented melting point. We attempted to confirm melting points rather than record freezing points due the fact that most malleable materials with solid-liquid thresholds in our temperature range were either highly volatile, or would supercool by a large amount before freezing. Similar methods have been used in previous studies to characterize cooling stages (Kanji and Abbatt, 2006). We chose to perform our experiments on mercury, which has a documented melting point of -38.83 °C (Lide, 2008) that is conveniently near the coldest end of the temperature range used in this study. The procedure used for the mercury melting experiments was identical to the aforementioned procedures, except that we shut off the humidified flow. For these experiments, the chamber was purged with dry nitrogen gas. As before, our experimental method consisted of us cycling the temperature at 1.0 ^{o}C/min, except this time the upper and lower temperature limits were

accordingly set to -60 °C and -30 °C in order for the mercury to completely freeze and melt, respectively. The data, as depicted in Figure 7, showed that melting occurred at -39.1 °C with a standard deviation of less than a tenth of a degree. For mercury, the temperature at which the melting process occurred was colder than the documented melting point by ~ 0.3 °C.

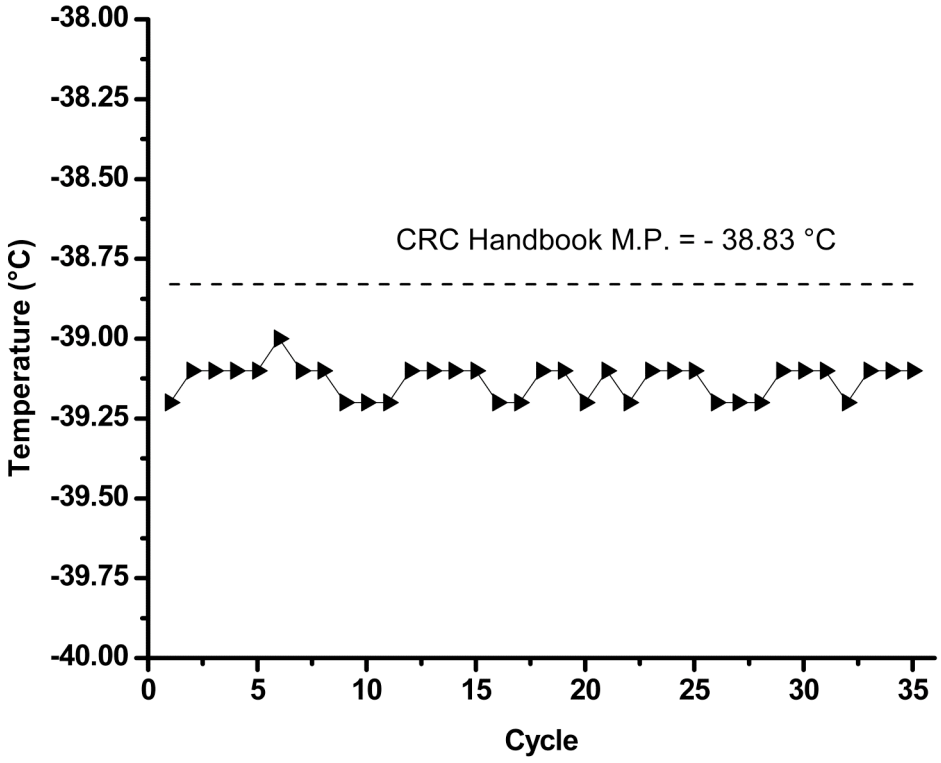

Figure 7: Our recorded temperatures for the observed melting point of mercury (triangles) in our setup are shown. The dashed line indicates the documented literature value for the melting point of mercury (Lide, 2007).

Our experiments with pure water droplets (HPLC grade) with a volume of 2.0 μL produced an average freezing temperature of -33.1 °C with a standard deviation of 0.6 °C.

These results correspond directly to the freezing temperatures reported in the literature for similar-sized droplets (Langham and Mason, 1958; Mason, 1971). This is an important result because it shows that contact with the silanized slides used in our experiments is not facilitating nucleation at warmer temperatures relative to those expected for the freezing of pure water in a laboratory study. These temperatures also confirm the purity of our water, because contamination, if present, could have caused freezing at higher temperatures.

Our experiments with mercury show a possible temperature offset of ~ 0.3 °C between our cooling stage's temperature sensor and our sample. Our freezing temperatures for pure water are in line with those from previous studies, but there is no quantifiable uncertainty that can be attributed to this data since many elements of these studies are not directly comparable to our study. Although we believe our visual detection method to be of high resolution and speed, we allow for a temperature uncertainty of 0.2 °C since we use only visual detection methods. Further, we allow for a 0.1 °C temperature uncertainty for any possible human error in the image analysis process. Thus, the freezing temperatures reported in this section are reported with a maximum uncertainty of ± 0.4 °C (this result is attained by taking the square root of the sum of squares of each individual uncertainty).

3.2 Ice Nuclei Behavior

Each IN type used in this study was unique in how it interacted with the respective water droplet. This behavior is directly related to the hydrophobic or hydrophilic tendencies, and thus the chemical composition, of each IN. Although it is

possible to position an IN anywhere in the droplet using significant force, each IN type had specific positions where they would come to rest. Then, based on which IN was being tested, it may or may not be able to be maneuvered to another position using the hypodermic syringe. Since we are concerned with gaining insights into atmospheric ice nucleation, we conducted experiments with regard to the natural behavior of the IN as it interacts with the water droplet because they represent events that are possible in the atmosphere.

Each time a volcanic ash particle was positioned on the surface of the droplet, it was immediately taken in by the droplet to the inside surface. Therefore, in the volcanic ash experiments, the IN was inside the droplet, and either in the middle of the droplet or in contact with the droplet surface. This change in position was possible because volcanic ash acted relatively neutral in the droplet, and could be moved with little effort to any desired position along the bottom of the droplet. It should be noted, though, that the volcanic ash IN used in this study would only allow for contact freezing experiments from the inside surface, and that attempts to move the IN to the outside of the droplet were not successful. However, there is previous evidence that contact freezing occurs at the same temperature regardless of whether the IN is in contact with a droplet's surface from the inside or the outside of a droplet (Durant and Shaw, 2005). The volcanic ash particles remained intact during experiments, so the only changes in the amount of contact between the IN and the droplet surface resulted from slight movements or rotations associated with the freezing and melting of the droplet. The volcanic ash particles are fragile after being used in the experiments, and so once an experiment was finished the particle could not be used again.

Interactions between peat soil particles and the surface of the water droplet varied from those with volcanic ash. Upon placing the peat IN at the droplet surface, the particle adhered to the droplet surface, with almost the entirety of the particle being outside the droplet. This adherence was significant enough to keep it attached to the droplet surface even if the slide was tilted or if the syringe was used to try and move the particle away from the droplet. If an attempt was made to move the particle to anywhere inside the bulk of the droplet, it promptly returned to its original position. Although it was possible to place the peat IN at any point on the perimeter of the droplet for contact freezing experiments, immersion experiments were not possible without severely damaging the IN. While the peat IN were not soluble in our water droplets, they did become slightly fragile as experiments progressed and would disperse some fragments into the droplet. There was no noticeable effect on freezing temperature as a result of this fragmentation.

Due to their high hydrophobicity, soot particles interacted with the surfaces of water droplets in a unique way as well. When placed at the interface of the water droplet, a soot particle would minimize its surface contact and subsequently stay completely outside the droplet for the entirety of the experiment. Similar to the peat IN, soot could not be moved inside the droplet without compromising the experiment. However, soot minimized its surface contact to such a degree that it could easily be moved away from the droplet, and the particle would fall away from the droplet if the slide were tilted. Despite the weak adherence of the soot to the droplet's outside surface, contact was maintained for the duration of our experiments.

3.3 Contact Freezing Versus Immersion Freezing

We sought to extend the results (Shaw et al., 2005; Durant and Shaw, 2005) that showed a definite difference in nucleating efficiency between a volcanic ash IN placed in the bulk of a water droplet and an IN placed in contact with the water-air interface. In order to do this, we set up five experiments with an IN at each position using volcanic ash.

In our five contact freezing experiments, with 25 cycles each, using volcanic ash as the IN, the average freezing temperature was -11.2 °C with a standard deviation of 1.0 °C. This compares to an average contact freezing temperature of between -17 °C and -18 °C in Shaw et al. (2005) and Durant and Shaw (2005).

In contrast, our five immersion freezing experiments using volcanic ash as the IN, the average freezing temperature was -18.3 °C with a standard deviation of 2.0 °C. This compares to a reported average immersion freezing temperature of approximately -22 °C in Shaw et al. (2005) and Durant and Shaw (2005).

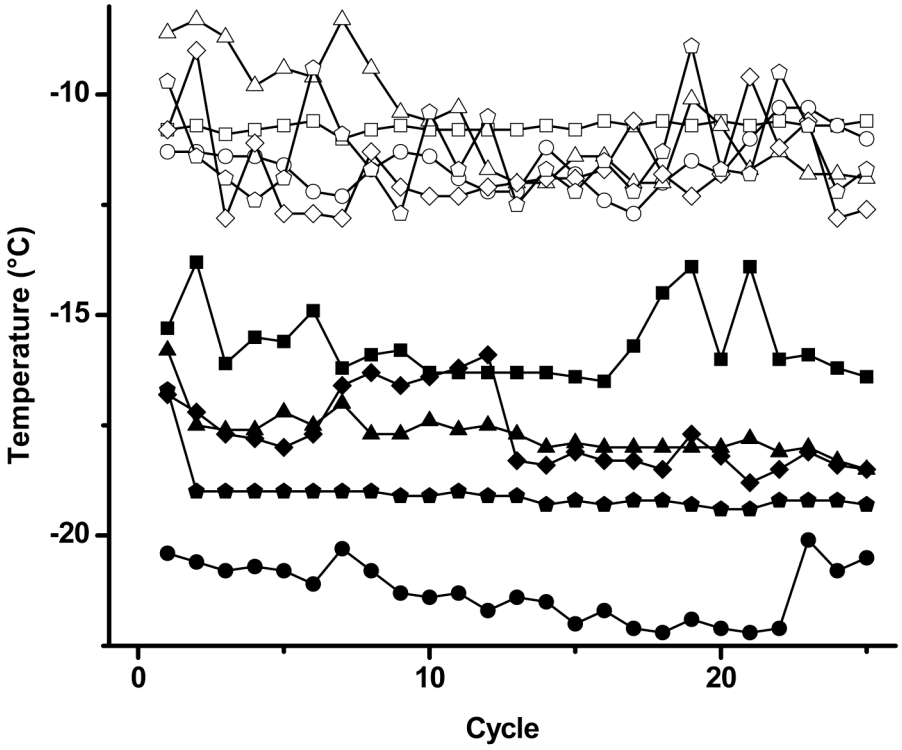

Figure 8: Recorded freezing temperatures are shown for all immersion freezing experiments (solid symbols) and all contact freezing experiments (open symbols) with volcanic ash as the IN.

These results are shown in Figure 9, and it can be seen that although there is some variability within the results for each mechanism, there is no overlap and the two mechanisms are significantly different. When the two modes from our results are compared, we see a significant difference in average freezing temperature of approximately 7 °C. This is larger than the difference reported by Shaw et al. (2005) and Durant and Shaw (2005) of 4 to 5 °C. We attribute key differences in experimental methodology to the difference between studies. Most notably, the cooling rate used in this study was 1 °C/min, whereas the previous studies used 10 °C/min. Our earlier

discussion revealed a significant offset in freezing temperature between these two cooling rates. Although this does not completely account for the differences in freezing point data, it could account for a majority of the temperature difference. However, the offsets due to their faster cooling rate could be even larger than this since they use a chamber of a much larger volume. The remaining difference could be attributed to differences in the composition and type of volcanic ash used as the IN (they do not report what kind it is) and a difference in size range for these IN (250-300 μm used here versus ~100-300 μm used in Shaw et al., 2005; Durant and Shaw, 2005). In addition, we performed a series of five experiments for each nucleation mode, with 25 freezing points in each experiment. Shaw et al. (2005) and Durant and Shaw (2005) use a single IN in a single experiment to gather many data points (~100) for a specific mode. Performing an analysis on a group of ten experiments with ten separate IN can possibly lead to different results than a study using one experiment and one IN would yield.

3.4 Contact Freezing Results as a Function of Composition

As stated previously, we conducted our contact freezing experiments using three different types of IN, which were Mount St. Helens volcanic ash, Pahokee Peat Soil II, and Carbon (Lampblack). Our experiments with IN were conducted using a constant droplet volume of 2.0 μL, and for experimental feasibility, the IN of each type are larger than those prevalent in the atmosphere. Specifically we used sieving to select IN within the size range of 250-300 μm. Experiments were conducted with all three types of IN until we had five complete experiments for each IN type. We analyzed the images from

these experiments and performed statistical analysis on all of the freezing point data that was extracted from them.

3.4.1 1980 Mount St. Helens Volcanic Ash

Analysis of the experiments run with Mount St. Helens volcanic ash as the IN showed that the average contact freezing temperature was -11.2 °C with a standard deviation of 1.0 °C. Our recorded freezing temperatures were in agreement with Mason and Maybank (1958), Isono et al. (1959), and Isono and Ikebe (1960), which showed that volcanic ash particles were capable of initiating freezing temperatures below -12 °C. However, significant caveats include that these studies did not distinguish contact freezing from other heterogeneous mechanisms and that the source volcanoes were different. Thus, no direct comparison with our measurements can be made.

During individual experiments we see relative consistency of the freezing points with respect to each other. However, when experiments using different particles of the same type are compared to each other, there is quite a bit of variability. There is roughly a five-degree spread of freezing temperatures (-8.3 °C to –12.8°C) when all of the ash data is pooled together. Note that volcanic ash was an external mixture with a high variability of relative chemical composition, yet our sieving techniques narrow this variability somewhat.

3.4.2 IHSS Pahokee Peat Soil II

The results from the experiments using peat as the IN showed it to be highly effective at facilitating freezing of the water droplets at higher temperatures, as they had

an average freezing temperature of -10.5 °C with a standard deviation of 1.8 °C. These freezing temperatures are in the same range as the volcanic ash IN. Our temperatures are consistent with Vali (1968), who showed that surface soils containing organic particles were capable of initiating freezing temperatures of as warm as -8 °C, and Schnell (1972,1974) who showed some which had freezing temperatures between -5 °C and -8 °C. However, there is no ice nucleation data available that specifically deals with humic acid IN, and so direct validation of our data is not possible.

There is an approximate six-degree range (-6.5 °C to -12.8 °C) of freezing temperatures for peat IN, but most of the freezing temperatures lay within the range of -9.5 °C to -12.8 °C. This, and the standard deviation, are affected by one experiment that had an average freezing temperature of -6.8 °C. We then performed an additional experiment to further characterize the statistical uniqueness of this single experiment, and thus we have six experiments instead of five in our data set. This experiment yielded data in the same range as the majority of the data with an average freezing temperature of -12.0 °C. Although the freezing points are statistical outliers when compared with the mean, we include this experiment in our data set because we do not know the reasons for the difference for certain.

3.4.3 Carbon (Lampblack)

Our experiments resulted in average contact freezing point temperatures of -25.6 °C with a pooled standard deviation of 3.4 °C. These temperatures are much lower than those observed for the other two types of IN, possibility due to the low amount of surface area contact the soot's chemical composition would allow. These heterogeneous

ice nucleation temperatures are consistent with values reported by Diehl et al. (1998). If valid, a direct comparison between traditional contact freezing and the contact freezing in this experiment would support our broadening of the definition for this mechanism. However, we note that although the measurements by Diehl et al. (1998) were contact freezing specific, their techniques make it possible that freezing observed in that study occurred via other mechanisms. The authors suggest the possibility of a hydrocarbon film on the droplet or IN surfaces that inhibits contact nucleation. Regardless, the qualitative results are consistent with several studies on soot as IN (DeMott, 1990; Möhler et al., 2005; Dymarska et al., 2006) and show soot to be a poor IN with ice nucleation temperatures below -25 °C.

The soot data set has the largest spread of freezing temperatures of approximately -13 °C (-18.8 °C to -31.7 °C), with most of the data lying in the range of -23.1 °C to -31.7 °C. Once again the spread and standard deviation are made larger by a single experiment with an average freezing temperature of -19.5 °C. We also performed one additional experiment with this IN because of this experiment, and it also produced freezing points that fell in with the majority of the data, with an average freezing temperature of -27.5 °C. We included all six data sets in our final analysis.

4. DISCUSSION

Our observed freezing temperatures collected for all IN compositions and mechanisms studied are shown in Figure 9 and Table 1.

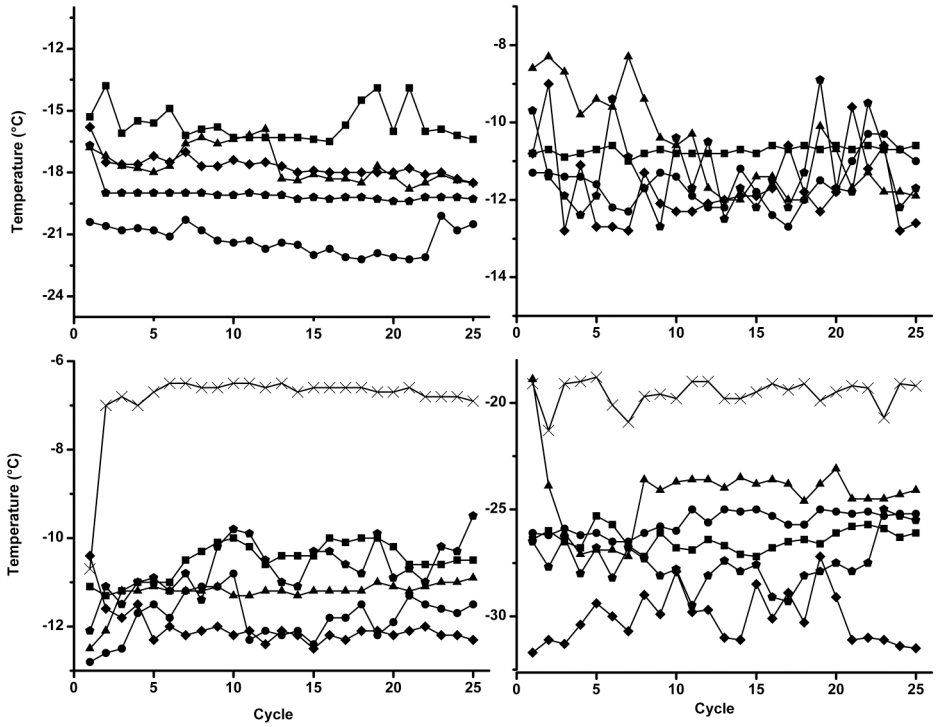

Figure 9: All of our freezing point data is shown for all four experimental groups. The upper-left graph shows our volcanic ash immersion freezing data, the upper-right graph shows our volcanic ash contact freezing data, the lower-left graph shows our peat contact freezing data, and the lower-right graph shows our soot contact freezing data.

Table 1: Recorded freezing temperatures are shown for all experiments with all types of IN and mechanisms.

	Average Freezing Temp. (^{o}C)	Std. Dev. (^{o}C)	No. of Expts.	No. of Freezing Events	Min. Freezing Temp. (^{o}C)	Max. Freezing Temp. (^{o}C)
Mt. St. Helens Ash Contact	-11.2	1.0	5	125	-12.8	-8.3
IHSS Pahokee Peat	-10.5	1.8	6	150	-12.8	-6.5
Carbon (Lampblack)	-25.6	3.4	6	150	-31.7	-18.8
Mt. St. Helens Ash Immersion	-18.3	2.0	5	125	-22.2	-14.5

We observed a definite difference between the two modes of freezing, and we find that difference to be larger than in the compared studies. We conducted five separate experiments that yielded 125 freezing points for each mode of nucleation. Although it is desirable to eliminate variables by using the same IN repeatedly, if a differently structured study were to produce the same qualitative difference in nucleation modes, then this difference between modes becomes a more consistent observation. In our study, both the size of the aerosol acting as IN and the volume of the droplet were carefully controlled for reproducible experiments.

We determined the contact freezing temperatures on IN of several different compositions, in order to evaluate which intrinsic particle properties influence the contact freezing processes. The average contact freezing temperatures observed for each IN type

are significantly different at the 95% confidence level. The Pahokee Peat Soil is the most effective IN and soot is the least effective IN. Although we have stated that the freezing efficiencies of volcanic ash IN and of peat IN are statistically different, a qualitative review of the results shows similarity in the two data sets. The freezing efficiency of soot IN is poor in comparison with peat and ash, as the freezing temperatures are much lower statistically and qualitatively. A direct and detailed comparison to previous results is difficult since previous measurements for contact freezing are very limited. However, a simple comparison to previous studies shows relatively consistent temperature ranges in which certain IN compositions are active in heterogeneous ice nucleation. More studies of this kind using different IN compositions are needed to adequately parameterize contact nucleation events occurring in the atmosphere.

The variability from particle to particle is apparent even within specific IN types. Table 1 contains freezing temperatures, standard deviations, and in the table it is clear that there is much variability between experiments on particles within the same IN composition in this study. This variability could be attributed to many things, including possible differences in experimental setup and differences in the intrinsic properties of the particles. Differences in experimental setup could include the positioning and preparation of both the droplet and particle on the slide prior to the experiment. In a preliminary study using our apparatus, a series of experiments was carried out in which a single particle was "re-used" (i.e. after a set of measurements a new droplet was added to the existing particle and another experiment was conducted). These attempts resulted in freezing temperatures within one degree of the original experiment. Thus, we believe the experimental setup does not produce a significant part of this variability due to attempts

to “re-use” a particular aerosol in multiple setups. The particle positioning within the droplet, which includes both the way in which the particle is oriented as well as the location inside or outside the droplet, is highly dependent on the chemical composition and physical size of the particle. This suggests that most of the variability in freezing temperatures between experiments comes from the characteristics of the particle itself rather than from any other source.

Differences in particle composition subsequently lead to possible differences in hydrophobicity, which can affect how a particle acts in positioning itself within a water droplet. For instance, a very hydrophobic particle will position itself to minimize its contact with the water droplet, possibly even keeping itself outside the droplet, as was the case with the soot particles. In addition, the particle’s size, especially relative to the size of the droplet, can affect where it will come to rest within the droplet. Particle size also affects how much available surface area of an IN is available to be in contact with the surface of a droplet. Finally, the shape and surface roughness of a particle are also important characteristics that can determine how much surface area is in contact with the droplet surface.

When attempting to find reasons for the differences in freezing efficiency and even the variability in results for one type of IN, these IN qualities must be taken into account. The soot IN had a weak attachment to the droplet surface since it is significantly hydrophobic. Because of this, we believe soot IN had more positional shifts during experiments than the other IN. This could have affected the amount of surface area in contact with the droplet surface, and thus caused more variability between soot IN than seen in the other experimental groups. Further, soot IN were hydrophobic and

limited their contact with the droplet surface so that some freezing temperatures were relatively close to those of pure water. The peat IN had a much stronger attachment to the droplet surface, and also much less variability between contact freezing experiments. Since our volcanic ash IN were always inside the droplets, yet could easily be moved with a hypodermic syringe, we believe that relatively moderate amounts of positional shifts were possible. They were not firmly fixed in one position on the droplet surface, yet were also only free to move in an environment that was denser than the air a soot IN was in. Thus, the variability in our ash experiments for both mechanisms had variability that was somewhere between that of the peat IN and soot IN groups.

4.1 Application of Classical Nucleation Theory

While it is well known that the presence of an object or nuclei can facilitate the freezing of a supercooled water droplet at warmer temperatures than the freezing of pure water, a complete mechanistic understanding of such heterogeneous nucleation events does not exist. In fact, over the last half-century there has been much disagreement on the theories and proposed mechanisms that govern heterogeneous nucleation by contact freezing alone. Despite much recent advancement in heterogeneous ice nucleation theory (Liu, 1999; Khvorostyanov and Curry, 2000, 2004, 2005; Chen et al., 2008), the classical nucleation theory equations from Fletcher (1962) remain the most-tested and widely-used method of quantifying heterogeneous ice nucleation. Although Fletcher (1970) states that these equations do not apply to contact freezing, he speaks of the mechanism in the traditional sense which involves a collision of the IN and droplet. In the case where the IN is constantly in contact with the surface of a droplet, these equations still apply.

In classical nucleation theory, the nucleation rate per particle is described by the following equation:

$$J = 4\pi r_N^2 K \exp\left[\frac{\Delta G^*}{k_B T}\right] \quad (1)$$

In this equation, r_N represents the radius of the IN, K represents the kinetic coefficient, ΔG^* represents the Gibbs free energy of the formation of a critical ice embryo on the surface of the IN, k_B represents the Boltzmann constant, and T represents the temperature in Kelvin (McDonald, 1964). Significant differences in nucleation rate can be caused by relatively small changes in the thermodynamics, or by very large changes in the kinetics. In other words, the Gibbs free energy term ΔG^* is the most variable term in the equation. Next, this general nucleation equation is modified for the case of heterogeneous nucleation of supercooled water (Fletcher, 1962).

As shown in Pruppacher and Klett (1997), and Fletcher (1962), the correct form for calculation of the single-particle nucleation rate according to classical theory is:

$$J \approx \frac{k_B T}{h} 4\pi r_N^2 n_c' \exp\left[-\frac{\Delta g}{RT} - \frac{\Delta G^*}{k_B T}\right] \quad (2)$$

Here the additional exponential term attempts to account for the activation energy (Δg) of water molecules diffusing across the solid-liquid interface, and the kinetic coefficient is further expanded where h is the Planck constant and n_c' is the number of water molecules in contact with a unit area of the IN surface (Turnbull and Fisher, 1949; Fletcher, 1962). The Gibbs free energy term still remains the most dominant value, and is defined as:

$$\Delta G^* = \frac{16\pi M_w^2 \sigma_{i/w}^3 f\left(m_{i/w}, x\right)}{3k_B T (n_i l_f)^2 \Delta T^2} \tag{3}$$

Here M_w represents the molecular weight of water, $\sigma_{i/w}$, represents the interfacial free energy per unit area between ice and liquid water (this is equivalent to the surface tension), f represents the wetting parameter, n_i represents the number of molecules per unit volume for ice, l_f is the latent heat of fusion for water, and ΔT is the difference between the melting point of water and the given temperature (Fletcher, 1962; Pruppacher and Klett, 1997).

In our experiments, all of these terms are the same, regardless of composition, with the exception of the wetting parameter, f. The wetting parameter is a function of both the size and composition of the IN. As shown above, f is a function of $m_{i/w}$, which is equivalent to the cosine of the contact angle, θ, between the IN substance and the ice embryo:

$$m_{i/w} = \cos\theta \tag{4}$$

In addition, f varies with x, which is equivalent to the ratio of IN radius, r, to the critical radius of the outer surface of a spherical-cap ice embryo, r^* (Fletcher, 1962; McDonald, 1964):

$$x = \frac{r}{r^*} \tag{5}$$

The formula for f is (Fletcher, 1962; Pruppacher and Klett, 1997):

$$f(m,x) = 1 + \left(\frac{1-mx}{\phi}\right)^3 + x^3\left[2 - 3\left(\frac{x-m}{\phi}\right) + \left(\frac{x-m}{\phi}\right)^3\right] + 3mx^2\left(\left(\frac{x-m}{\phi}\right) - 1\right) \tag{6}$$

where

$$\phi = (1 - 2mx + x^2)^{\frac{1}{2}} \quad (7)$$

Based on the equations above, for IN of a certain size, a substance with a higher contact angle will subsequently have a higher corresponding wetting parameter. A higher wetting parameter results in a smaller value for nucleation rate, which means that an IN with a smaller *f* parameter will be more efficient at nucleating ice than an IN with a larger *f* parameter. In contrast, changing the size of the IN and thus changing the *x* parameter has very little effect upon changing the magnitude of *f*. These equations will be used for calculating the single particle heterogeneous nucleation rate in the next section. Today there remains much debate as to how appropriate and accurate it is to apply classical nucleation theory to heterogeneous processes (Eastwood et al., 2008).

4.2 Probability of Freezing

Probability is traditionally used to describe ice nucleation because ice nucleation has been theorized to be a stochastic process. Given the large number of freezing points collected in our experiments, we can use the collective data sets for each composition to generate an 'empirical' probability of freezing as a function of temperature for droplets set up with each composition of IN (Shaw et al., 2005). Figure 11 shows our data in terms of the probability that a droplet would have frozen at a certain temperature for a given IN type. For instance, out of 150 total contact freezing events recorded for soot, a number of them will be observed to have frozen by a given temperature. This empirical probability of freezing is related to the nucleation rate in the following manner:

$$P \equiv \frac{N_f}{N_0} = 1 - \exp\left(-\int_0^t J dt\right) \tag{8}$$

Here, N_0 is defined as the total number of droplets, N_f is defined as the number of those droplets which have frozen at a certain temperature, J is the heterogeneous nucleation rate, and t is the time elapsed over an experiment (Shaw et al., 2005). Even though there is variability in freezing temperatures as previously discussed, overall the freezing is likely to occur over a relatively narrow range for a specific IN type. The likelihood that an IN will induce freezing is highly dependent upon composition and mechanism, which can be seen in Figure 11.

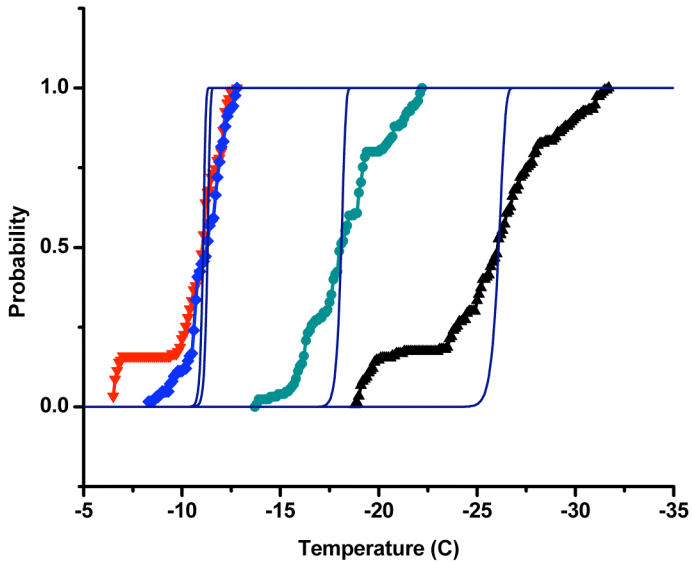

Figure 10: All recorded freezing temperatures are shown as data points along the empirical freezing probability curves. The curves represent the probability (y-axis) that a water droplet with a certain IN type will have frozen at a given temperature (x-axis). The left-most (red) curve represents the peat contact freezing experiments, the next (blue) curve represents the volcanic ash contact freezing experiments, the next (green) curve represents the volcanic ash immersion freezing experiments, and the right-most (black) curve represents the carbon (lampblack) contact freezing experiments. The fitted curves (navy) represent the calculated theoretical freezing probability of an IN of each experimental group.

Using the classical nucleation equations and the mathematical relation between the nucleation rates and empirical freezing probability, we can create theoretical probability curves for IN with estimated parameters similar to those IN used in our experiments. Many of the estimated values that are entered into the equations come from Pruppacher and Klett (1997). These curves can then be fitted at the 50% probability levels to our empirical probability curves in order to estimate the numerical value of the wetting parameter, *f*, for the IN compositions and mechanisms in this study (Shaw et al., 2005). These fitted theoretical curves are also in Figure 10.

As discussed, when all of the freezing data is grouped together for each IN composition and mechanism, then we can produce the empirical probability curves seen in Figure 10. When we fit the theoretical curves from classical nucleation theory to these empirical curves at the 50% probability level, we get *f* values of 0.093 for peat contact freezing, 0.097 for volcanic ash contact freezing, 0.251 for volcanic ash immersion freezing, and 0.537 for soot contact freezing.

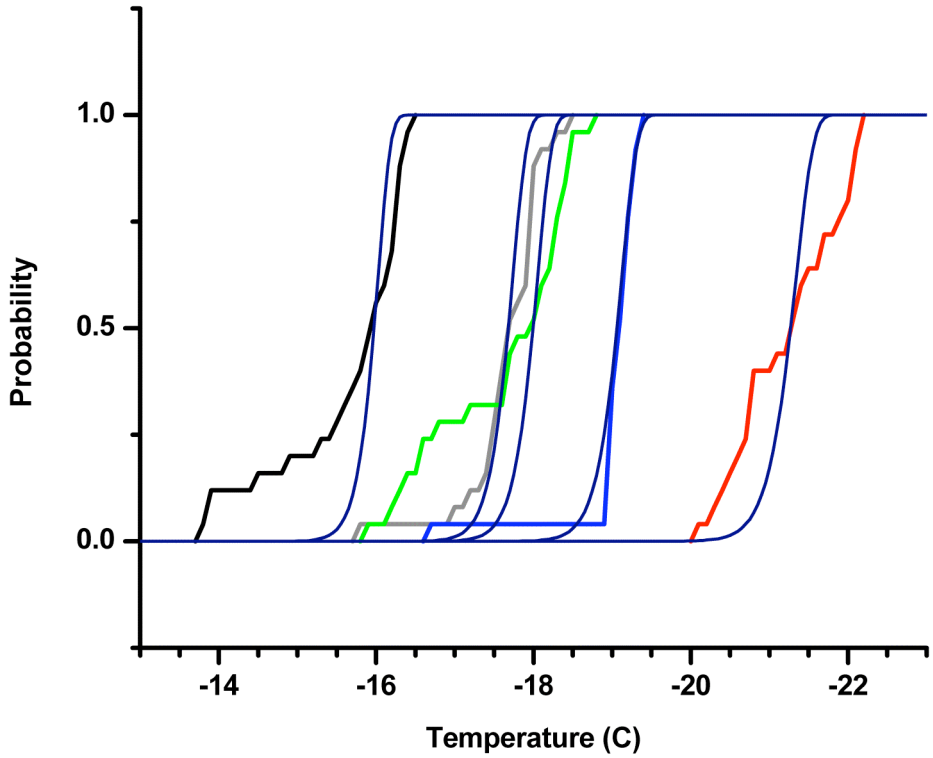

Figure 11: The empirical freezing probability curves (various colors) for one experimental group, volcanic ash immersion freezing, are shown with their fitted theoretical probability curves.

However, since each experiment uses a different IN with possibly different wetting parameters, we deem it more appropriate to perform this method of estimating *f* with each separate experiment. The empirical and theoretical probability curves for all five volcanic ash immersion experiments are shown in Figure 11. As it can be seen, the empirical curves for individual experiments match their corresponding theoretical curves much more closely than the curves in Figure 10. Additionally, we attain five *f* values for each composition and mechanism rather than assigning a single f value to five separate

IN. For each group of freezing experiments, we report the range of acquired wetting parameter values in Table 2.

In our application of classical nucleation theory to our results, the efficiencies of each type of IN and mechanism are quantified further. When all experiments are grouped together by composition or mechanism, we can see that the total *f* values are lowest for the peat contact freezing experiments, followed by volcanic ash contact freezing, volcanic ash immersion freezing, and soot contact freezing, in order. However, as we noted earlier, we thought it was more appropriate to calculate the *f* values for each individual experiment due to our methodology. We then report the range of *f* values, as well as the average and median f value for each group in Table 2. In doing so our data set shows the relative difference in nucleating efficiencies between groups, as well as the variability of freezing efficiency with each group. Here we again see peat contact and ash contact to be quite close in nucleating efficiency, yet we see that the ash immersion and soot contact experimental groups are shown to be much less efficient at nucleating ice.

Table 2: The calculated *f* values are shown for all types of IN and mechanisms.

	No. of Expts.	Grouped *f*	Individual *f* Range	Average *f* for Individual Experiments	Median *f* for Individual Experiments
Mt. St. Helens Ash Contact	5	0.097	0.087 to 0.108	0.098	0.101
IHSS Pahokee Peat	6	0.093	0.032 to 0.111	0.086	0.092
Carbon (Lampblack)	6	0.537	0.290 to 0.741	0.526	0.483
Mt. St. Helens Ash Immersion	5	0.251	0.196 to 0.351	0.263	0.248

Significantly, we also find a large difference in nucleating efficiency between contact freezing and immersion freezing using volcanic ash IN regardless of whether we examine total *f* values or individual experiment *f* values. Seeing that the same type of IN was used in order to compare the mechanisms, we must re-examine the mathematical definition of the wetting parameter, *f*. The wetting parameter is a function of both *m*, which is equal to the cosine of the contact angle between the specific IN and the ice embryo, and also *x*, which is a function of both the size of the IN and the critical size of the ice embryo. In this understanding, the contact angle would not change between IN of the same composition. However, the critical size of the ice embryo needed would be lower at the water-air interface than in would in the bulk of the droplet (Djikaev et al., 2002). Lowering this critical size would increase the size of *x*, which in turn would lower the size of the wetting parameter, *f*. Our observations are consistent with these qualitative arguments, though as we noted earlier, a change in x does not change the f value

significantly. Our results for f values show a significant numerical difference between the mechanisms of contact and immersion freezing. Thus, the critical ice embryo size is reduced quite significantly when comparing contact freezing to immersion freezing, or the classical nucleation theory equations does a poor job in characterizing these heterogeneous ice nucleation processes. More work must be done before a definitive answer can be reached, but significant advances in ice nucleation theory must be made in order to successfully understand these atmospheric processes.

4.3 Heterogeneous Nucleation Rates and Contact Angles

Although our previous discussion of classical nucleation theory and *f* values involved a significant amount of assumptions and uncertainty, it is possible to continue this treatment further and report heterogeneous nucleation rates and contact angle values. Despite values for homogeneous ice nucleation rates being reliable and relatively consistent between different studies, heterogeneous nucleation rates are rarely reported due to the difficulties and uncertainties in deriving these values (Pruppacher and Klett, 1997). In studies where they are calculated and reported (DeMott, 1995; Hung et al., 2003; Archuleta et al., 2005; Kanji and Abbatt, 2006, 2008; Pant et al., 2006; Eastwood et al., 2008) the values can vary as much as by six orders of magnitude. This is in part expected since rates depend theoretically on a number of factors including mechanism, temperature, relative humidity, IN composition and size, and droplet size. Much more work must be done in this field in order to rectify these issues, as heterogeneous nucleation rates, particularly ones that are mechanism-specific, are highly important in describing how prevalent these processes are in the atmosphere.

Different methodologies in both experimentation and calculations of heterogeneous nucleation rates account for much of the variability in these reported values. Though there are few rates reported for the mechanisms of contact freezing and immersion freezing, it is important to note that the calculation techniques used here for our investigations of contact freezing differ from those for collisional contact freezing because our calculations do not involve collisions. Thus, Brownian collection of IN particles by droplets used in the calculation of rates in DeMott et al. (1983), DeMott (1995), and Finnegan (1998), which is likely to be the rate-limiting step in studies examining collisional contact freezing, is not incorporated into our rates.

We calculate rates by first finding the corresponding *f* value using the fitting process described earlier for a particular set of experimental data. For reasons described in Section 4.2, we use the average *f* value for individual experiments within each mechanism or IN type. Equation 2 in Section 4.1 shows the calculations necessary for single-particle heterogeneous nucleation rates. For the heterogeneous nucleation rate for an IN population, the surface area term ($4\pi r^2$) is removed from Equation 2 and the calculation is performed using the appropriate *f* value.

Due to the constraints of the classical nucleation theory used here, heterogeneous nucleation rates are identical for each experimental group at a given ratio of freezing. Although each group may have a unique *f* value, the theoretical probability curves calculated by classical nucleation theory are simply translated left or right depending on the change in f value, but remain identical in shape. As an example, for volcanic ash contact freezing, which had an average *f* value of 0.098, the rate of heterogeneous freezing was ~ 2.8×10^{-3} cm^{-2} sec^{-1} at the 50% probability level. Volcanic ash immersion

freezing has an identical nucleation rate at the 50% probability level, but the temperature at which the 50% probability level occurs is different for each. Thus, from our calculations it is only possible to compare the heterogeneous nucleation rates of each experimental group at a specific temperature and thus assess their relative nucleation efficiencies. Our reported heterogeneous nucleation rates are shown in Figure 12.

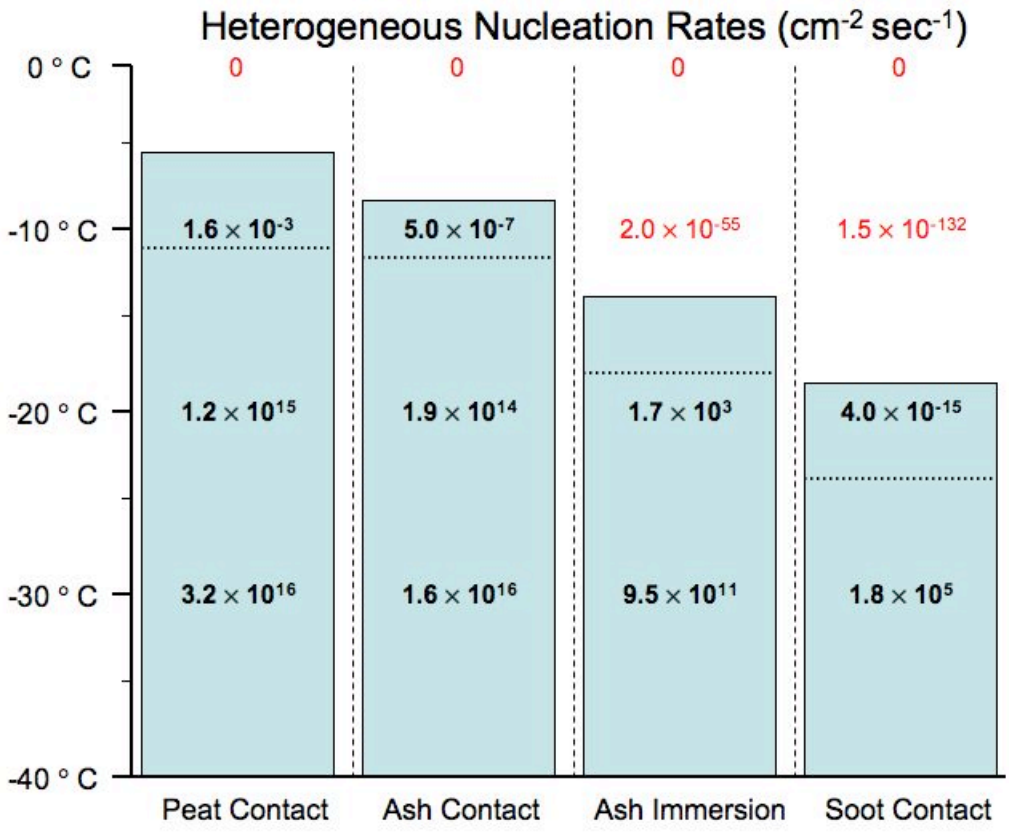

Figure 12: Our calculated heterogeneous nucleation rates are shown. The blue regions represent the temperature range over which a specific experimental group would be active as IN according to our experimental data. Subsequently, rates in red indicate that there is no ice nucleation occurring in our experimental data, while rates in black indicate that there is ice nucleation occurring. The horizontal dotted lines within the blue regions indicate the temperature at which 50% of our freezing events had occurred.

We can also calculate specific values for the contact angle between the ice embryo and IN surface by taking advantage of a simplification for the calculation of *f* values. In instances where the radius of the IN far exceeds the radius of the critical ice embryo, the formula for *f* becomes (Fletcher, 1962; Pruppacher and Klett, 1997):

$$f(m,x) = \frac{m^3 - 3m + 2}{4} \tag{9}$$

By solving for m and using Equation 4, the contact angle value can be calculated for any corresponding *f* value. These values are reported in Table 3.

Table 3: The calculated θ values are shown for all types of IN and mechanisms.

	No. of Expts.	Grouped θ	Individual θ Range	Average θ for Individual Experiments	Median θ for Individual Experiments
Mt. St. Helens Ash Contact	5	52.063	50.453 to 53.720	52.153	52.678
IHSS Pahokee Peat	6	51.432	38.220 to 54.154	49.714	51.267
Carbon (Lampblack)	6	92.830	73.264 to 109.495	92.027	92.487
Mt. St. Helens Ash Immersion	5	69.771	64.389 to 78.382	70.696	69.492

The calculated contact angle values differ greatly in range from those reported in Eastwood et al. (2008) for deposition onto mineral dust. Although two different heterogeneous mechanisms are being examined and different IN compositions are being used, both our data and the data from Eastwood et al. (2008) are calculated using classical nucleation theory and should agree somewhat. The discrepancies are primarily

due to the calculation and use of experimental nucleation rate values by Eastwood et al. (2008), which range from 1 cm^{-2} sec^{-1} to 22000 cm^{-2} sec^{-1}. The authors calculate their experimental heterogeneous nucleation rates based on the estimated number of ice crystals observed, the estimated surface area available for deposition, and the observation time, and then they solve for *f* by substituting their estimated rates into the classical nucleation theory equations. We find our f values by employing the Shaw et al. (2005) fitting technique, which has inherent limitations that can be seen in the curve fittings in Figures 11 and 12, but the results are still of significant value to this study. As we have stated, any result that is derived by applying classical nucleation theory to heterogeneous processes inherently has great amounts of uncertainty attributed to it, and this is the case with both the values in Table 3 and the values derived by Eastwood et al. (2008). The discrepancies may indicate that classical nucleation theory cannot adequately describe deposition, contact, and immersion freezing, or that one or more assumptions used by Eastwood et al. (2008), or by us, is more appropriate.

5. CONCLUSIONS AND IMPLICATIONS

In this study, the contact and immersion freezing temperatures of droplets induced by atmospherically relevant aerosols are measured. This study provides a direct comparison between the ice nucleating efficiencies of two heterogeneous ice nucleation mechanisms, as well as direct comparisons between three different IN compositions for a particular mechanism: Carbon (Lampblack), Mount St. Helens Volcanic Ash, and IHSS Pahokee Peat Soil II. In our comparison of contact freezing versus immersion freezing using volcanic ash as the IN, we observed an average contact freezing temperature of -11.2 °C ± 1.0 °C and an average immersion freezing temperature of -18.3 °C ± 2.0 °C. In both experimental results and qualitative analysis of heterogeneous ice nucleation theory, we supported the conclusions of Shaw et al. (2005) and Durant and Shaw (2005), which called for a broadened definition of contact freezing to include the surface-initiated freezing caused by an IN being in constant contact with the surface of a water droplet. In our comparison of three IN compositions using the same heterogeneous mechanism, Pahokee Peat Soil II particles were the most effective IN with an average contact freezing temperature of -10.5 °C ± 1.8 °C, followed by Mount St. Helens volcanic ash with an average contact freezing temperature of -11.2 °C ± 1.0 °C, and then carbon (lampblack) with an average contact freezing temperature of -25.6 ± 3.4 °C.

This is the first study of mechanism-specific freezing events that involves aerosols such a variety of well-characterized compositions as explored here. We found that, in terms of IN efficiency, peat soil raised the freezing temperature of a water droplet

the most, followed closely by volcanic ash. Carbon (lampblack) particles were the most hydrophobic particles included in the study and were found to be the least active as IN.

In our application of classical nucleation theory to our data set, we further characterized the nucleation efficiency of each IN type and mechanism by finding *f* values for each experimental group. In comparing these values, we found further evidence for a large difference in nucleating efficiency between immersion freezing and contact freezing. We also found further quantification of the nucleating efficiency of three different IN compositions under the contact freezing mechanism. These results were then extended to heterogeneous nucleation rates and contact angle values.

Better data on the temperatures at which heterogeneous ice nucleation occurs can lead to much better cloud models, which can produce much better models regarding Earth's radiative budget. Measurements of exactly how well a certain type of aerosol acts as an IN are also needed to characterize the relative impacts of anthropogenic aerosols on atmospheric processes that have an effect on Earth's climate. The numerical parameters found in our analysis of the freezing point data can assist atmospheric modelers in more accurately characterizing the processes of heterogeneous ice nucleation in the atmosphere.

Further, our study attempts to isolate single heterogeneous ice nucleation mechanisms in order to assess their characteristic nucleating abilities. Few heterogeneous ice nucleation studies have done this, yet it is vital that we have individual mechanism properties in order to understand ice nucleation in the atmosphere. We believe that our data set provides some key pieces of information to atmospheric scientists that may allow for a better understanding of atmospheric ice nucleation.

REFERENCES

Ansmann, A., I. Mattis, D. Müller, U. Wandinger, M. Radlach, and D. Althausen (2005), Ice formation in Saharan dust over central Europe observed with temperature/humidity/aerosol Raman lidar, *J. Geophys. Res*., *110*(D18S12).

Archuleta, C. M., P.J. DeMott, and S.M. Kreidenweis (2005), Ice nucleation by surrogates for atmospheric mineral dust and mineral dust/sulfate particles at cirrus temperatures, *Atmos. Chem. Phys*., *5*(3), 2617–2634.

Aronov, D., Rosenman, G., and Barkay, Z. (2007), Wettability study of modified silicon dioxide surface using environmental scanning electron microscopy, *J. Applied Phys.*, *101*(8), 084901.

Baker, B. A., and R. P. Lawson (2005), In situ observations of microphysical properties of wave, cirrus and anvil clouds. Part 1: Wave clouds, *J. Atmos. Sci., 63*(12), 3160–3185.

Beard, K. V. (1992), Ice initiation in warm-base convective clouds: An assessment of microphysical mechanisms, *Atmos. Res., 28*(2), 125– 152.

Bertram, A. K., D. D. Patterson, and J. J. Sloan (1996), Mechanisms and temperatures for the freezing of sulfuric acid aerosols measured by FTIR extinction spectroscopy, *J. Phys. Chem.*, *100*(6), 2376-2383.

Bigg, E. K., C. Leck, and L. Tranvik (2004), Particulates of the surface microlayer of open water in the central Arctic Ocean in summer, *Marine Chem.*, *91*(1-4), 131-141.

Brantley, S., and B. Myers (2000), Mount St. Helens - From the 1980 eruption to 2000 (Fact Sheet #036-00). U.S. Department of the Interior, *U.S. Geological Survey*, Vancouver, WA.

Brooks, S. D., P. J. DeMott, and S. M. Kreidenweis (2004), Water uptake by particles containing humic materials and mixtures of humic materials with ammonium sulfate, *Atmos. Environ.*, *38*(13), 1859-1868.

Chang, H. Y. A., T. Koop, and M. J. Molina (1999), Phase transitions in emulsified HNO3/H2O and HNO3/H2SO4/H2O solutions, *J. Phys. Chem. A*, *103*(15), 2673-2679.

Chelf, J. H., and S. T. Martin (1999), Laboratory measurements of H2O vapor pressures and equilibrium freezing temperature of aqueous NH4HSO4 solution from -30°C to 20°. *Geophys. Res. Lett., 26*(15), 2391-2394.

Chen, J.-P. A. Hazra, and Z. Levin (2008), Parameterizing ice nucleation rates for cloud modeling using contact angle and activation energy derived from laboratory data, *Atmospheric Chemistry and Physics Discussions*, *8*, 14419-14465, 29-7-2008.

Chen, Y., S. M. Kreidenweis, L. M. McInnes, D. C. Rogers, and P.J. DeMott (1999), Single particle analyses of ice nucleating aerosols in the upper troposphere and lower stratosphere. *Geophys. Res. Lett., 25*(9), 1391-1394.

Chughtai, A. R., M. E. Brooks, and D. M. Smith (1996), Hydration of black carbon. *J. Geophys. Res.*, *101*(D14), 19505-19514.

Cooper, W. A. (1974), A Possible Mechanism for Contact Nucleation, *J. Atmos. Sci.*, *31*(7), 1832-1837.

Cooper, W.A., and G. Vali (1981), The Origin of Ice in Mountain Cap Clouds*, J. Atmos. Sci., 38*(6), 1244–1259.

Cooper, W. A. (1986), Ice initiation in natural clouds, in *Precipitation Enhancement- A Scientific Challenge*, edited by R. G. Braham Jr., *Meteorol. Monogr., 443*, 29– 32.

Cooper, W. A. (1995), Ice formation in wave clouds: Observed enhancement during evaporation, *Proc. Conf. Cloud Physics*, Am. Meteorol. Soc., pp. 147–152, Dallas, TX.

Cotton, R. J., and P. R. Field (2002), Ice nucleation characteristics of an isolated wave cloud, *Q. J. R. Meteorol. Soc*., *128*(585), 2417– 2437.

Cziczo, D. J., and J. P. D. Abbatt (1999), Deliquescence, efflorescence and supercooling of ammonium sulfate aerosols at low temperature: Implications for cirrus cloud formation and aerosol phase in the atmosphere. *J. Geophys. Res.,104*(D11), 13,781-13,790.

DeMott, P. J. (1990), An exploratory study of ice nucleation by soot aerosols, *J. Appl. Meteor.*, *29*(10), 1072-1079.

DeMott, P. J. (1995), Quantitative descriptions of ice formation mechanisms of silver iodide-type aerosols, *Atmos. Res., 38*(1), 63–99.

DeMott, P. J. (2000), Laboratory studies of cirrus cloud processes, in *Cirrus*, edited by D. K. Lynch et al., pp. 102– 135, Oxford Univ. Press, NY.

DeMott, P. J., W.G. Finnegan, and L.O. Grant (1983), An Application of Chemical Kinetic Theory and Methodology to Characterize the Ice Nucleating Properties of Aerosols Used for Weather Modification*. J. Appl. Meteor., 22*(7), 1190–1203.

DeMott P. J., M.P. Meyers, W.R. Cotton (1994), Parameterization and impact of ice initiation processes relevant to numerical-model simulations of cirrus clouds, *J. Atmos. Sci*., *51*(11), 77-90.

DeMott, P. J. (1995), Quantitative descriptions of ice formation mechanisms of silver iodide-type aerosols, *Atmos. Res., 38*(1), 63–99.

Deshler, T., and G. Vali (1992), Atmospheric concentrations of submicron contact-freezing nuclei, *J. Atmos. Sci*., *49*(9), 773–784.

Diehl, K., and S.K. Mitra (1998), A laboratory study of the effects of a kerosene-burner exhaust on ice nucleation and the evaporation rate of ice crystals. *Atmospheric Environment, 32*(18), 3145-3151.

Diehl, K., S. Matthias-Maser, R. Jaenicke, and S.K. Mitra (2002), The ice nucleating ability of pollen: Part II. Laboratory studies in immersion and contact freezing modes, *Atmos. Res., 61*(2), 125–133.

Dinar, E., et al. (2006), Cloud condensation nuclei properties of model and atmospheric HULIS, *Atmos. Chem. Phys. Discuss.*, *6*(1), 1073-1120.

Djikaev, Y. S., A. Tabazadeh, P. Hamill, and H. Reiss (2002), Thermodynamic conditions for the surface-stimulated crystallization of atmospheric droplets, *J. Phys. Chem. A*, *106*(43), 10247–10253.

Djikaev Y. S., A. Tabazadeh, and H. Reiss (2003), Thermodynamics of crystal nucleation in multicomponent droplets: Adsorption, dissociation, and surface-stimulated nucleation, *J. Chem. Phys. 118*(14), 6572-6581.

Durant, A. J., and R. A. Shaw (2005), Evaporation freezing by contact nucleation inside-out, *Geophys. Res. Lett.*, *32*(L20184).

Duft, D. and T. Leisner (2004), Laboratory evidence for volume- dominated nucleation of ice in supercooled water microdroplets*, Atmos. Chem. Phys*., *4*(7), 1997–2000.

Dymarska, M., Murray, B. J., Sun, L., Eastwood, M. L., Knopf, D. A., and Bertram, A. K. (2006), Deposition ice nucleation on soot at temperatures relevant for the lower troposphere, J. Geophys. Res., *111*(D04204).

Eastwood, M. L., S. Cremel, C. Gehrke, E. Girard, and A. K. Bertram (2008), Ice nucleation on mineral dust particles: Onset conditions, nucleation rates and contact angles, J. Geophys. Res., *113*(D22203).

Field, P. R., et al. (2001), Ice nucleation in orographic wave clouds: Measurements made during INTACC, *Q. J. R. Meteorol. Soc., 127*(575), 1493–1512.

Finnegan, W. G. (1998), Rates and mechanisms of heterogeneous ice nucleation on silver iodide and silver chloroiodide particulate aerosols. *J. Colloid Interface Sci., 202*(2)**,** 518–526.

Fletcher, N. H. (1962), *The Physics of Rainclouds*, 386 pp., Cambridge University Press, Cambridge, UK.

Fletcher, N. H. (1968), Ice nucleation behavior of silver iodide smokes containing a soluble component. *J. Atmos. Sci*., *25*(6), 1058-1060.

Fletcher, N. H. (1969), Active sites and ice crystal nucleation, *J. Atmos. Sci*. *26*(6), 1266-1271.

Fletcher, N. H. (1970), On Contact Nucleation*, J. Atmos. Sci.*, *27*(7), 1098–1099.

Fruchter, J. S., et al. (1980), Mount St Helens Ash from the 18 May 1980 Eruption: chemical, physical, mineralogical, and biological properties., *Sci.*, *209*(4461), 1116-1125.

Fukuta, N. (1975), Comments on "A Possible Mechanism for Contact Nucleation". *J. Atmos. Sci., 32*(12), 2371–2373.

Fukuta, N. (1975), A Study of the mechanism of contact ice nucleation, *J. Atmos. Sci.*, *32*(8), 1597-1603.

Garrett, T. J., H. Gerber, D. G. Baumgardner, D. G., C. H. Twohy, and E. M. Weinstock (2003), Small, highly reflective ice crystals in low-latitude cirrus, *Geophys. Res. Lett.*, *30*(21), 2132.

Gokhale, N.R., and J. Goold (1968), Droplet Freezing by Surface Nucleation. *J. Appl. Meteor., 7*(5), 870–874.

Gokhale, N.R., and O. Lewinter (1971), Microcinematographic Studies of Contact Nucleation, *J. Appl. Meteor., 10*(3), 469–473.

Gokhale, N.R., and J.D. Spengler (1972). Freezing of Freely Suspended, Supercooled Water Drops in a Large Vertical Wind Tunnel, *J. Appl. Meteor., 11*(7), 1101–1107.

Gorbunov, B., A. Baklanov, N. Kakutkina, H. L. Windsor, and R. Toumi (2001), Ice nucleation on soot particles, *J. Aerosol Sci., 32*(2), 199–215.

Graber, E. R., Y. Rudich (2006), Atmospheric HULIS: how humic-like are they? A comprehensive and critical review, *Atmospheric Chemistry and Physics, 6*(3), 729–753.

Hobbs, P. V. (1993), Aerosol-cloud interactions, in *Aerosol-Cloud-Climate Interactions*, edited by P. V. Hobbs, pp. 33-73, Academic, San Diego, CA.

Hobbs, P.V., and A.L. Rangno (1985), Ice Particle Concentrations in Clouds. *J. Atmos. Sci., 42*(23), 2523–2549.

Hung, H.-M., A. Malinowski, and S. T. Martin (2003), Kinetics of heterogeneous ice nucleation on the surfaces of mineral dust cores inserted into aqueous ammonium sulfate particles, *J. Phys. Chem. A*, *107*(9), 1296 –1306.

IPCC (2007) *Climate Change 2007: The Physical Science Basis. Summary for Policy Makers. Contribution of Working Group I to the Fourth Assessment Report of the Intergovernmental Panel for Climate Change.* IPCC Secretariat, Geneva. 21 pp.

Isono, K., M. Komabayashi, and A. Ono (1959), The nature and origin of ice nuclei in the atmosphere, *J. Meteorological Society of Japan*, *37*, 211-233.

Isono, K., and Y. Ikebe (1960), On the ice-nucleating ability of rock-forming minerals and soil particles, *J. Meteorological Society of Japan*, *38*, 213-230.

Jaenicke, R., Tropospheric aerosols, in *Aerosol-Cloud-Climate Interactions*, edited by P. V. Hobbs, pp. 1 –31, Academic, San Diego, CA.

Jensen, E. J., and O. B. Toon (1992), The potential effects of volcanic aerosols on cirrus cloud microphysics, *Geophys. Res. Lett., 19*(17*)*, Pages: 1759-1762.

Jensen, E. J., and O. B. Toon (1997), The potential impact of soot particles from aircraft exhaust on cirrus clouds, *Geophys. Res. Lett.*, *24*(3), 249-252.

Kanji, Z. A., and J. P. D. Abbatt (2006), Laboratory studies of ice formation via deposition mode nucleation onto mineral dust and n-hexane soot samples, *J. Geophys. Res.*, *111*(D16204).

Kanji, Z. A., O. Florea, and J. P. D. Abbatt (2008), Ice formation via deposition nucleation on mineral dust and organics: dependence of onset relative humidity on total particulate surface area, *Env. Res. Lett*., *3*(2), 025004.

Kay, J.E., V. Tsemekhman, M. Baker, and B. Swanson (2003), Comment on evidence for surface-initiated homogeneous nucleation, *Atmos. Chem. Phys., 3*(5), 1439-1443.

Koop, T., H. P. Ng, L. T. Molina, M. J. Molina (1998), A new optical technique to study aerosol phase transitions: The nucleation of ice from H2SO4 aerosols. *J. Physical Chem. A, 102*(45). 8924-8931.

Khvorostyanov, V. I., and J. A. Curry (2000), A new theory of heterogeneous ice nucleation for application in cloud and climate models, Geophys. Res.

Lett., *27*(24), 4081–4084.

Khvorostyanov, V. I., and J. A. Curry (2004), The theory of ice nucleation by heterogeneous freezing of deliquescent mixed CCN. Part I: Critical radius, energy, and nucleation rate. *J. Atmos. Sci., 61*(22), 2676–2691.

Khvorostyanov, V. I., and J. A. Curry (2005) The theory of ice nucleation by heterogeneous freezing of deliquescent mixed CCN. Part II: Parcel model simulation. *J. Atmos. Sci., 62*(2), 261–285.

Krämer, B. H., O. Hübner, H. Vortisch, L. Wöste, T. Leisner, M. Schwell, E. Rühl, H. Baumgärtel (1999), Homogeneous nucleation rates of supercooled water measured in single levitated microdroplets. *J. Chem. Physics 111*(14), 6521-6527.

Langham, E. J. and B. J. Mason. (1958), The heterogeneous and homogeneous nucleation of supercooled water. *Proc. Roy. Soc. London A, 247*(1251), 493-504.

Lawson, R.P., B. Baker, B. Pilson, and Q. Mo (2006), In situ observations of the microphysical properties of wave, cirrus, and anvil clouds. part II: cirrus clouds. *J. Atmos. Sci*., *63*(12), 3186–3203.

Levin, Z., and S. A. Yankofsky (1983), Contact versus immersion freezing of freely suspended droplets by bacterial ice nuclei, *J. Applied Meteorology*, *22*(11), 1964-1966.

Lide, D. R. (Ed.) (2008), *CRC Handbook of Chemistry and Physics*, 89th edition, 2688 pp., CRC Press, Boca Raton, FL.

Liu, X. Y. (1999), A new kinetic model for three-dimensional heterogeneous nucleation. *J. Chem. Phys. 111*(4), 1628.

Lohmann, U. (2002), Possible aerosol effects on ice clouds via contact nucleation. *J. Atmos. Sci*., *59*(3), 647–656.

Mason, B. J., and J. Maybank (1958), Ice-nucleating properties of some natural mineral dusts, *Q. J. R. Meteorol. Soc.*, *84*(361), 235-241.

Mason, B. J. (1960), Ice-nucleating properties of clay minerals and stony meteorites, *Q. J. R. Meteorol. Soc.*, *86*(370), 552-556.

Mason, B. J., 1971: *The Physics of Clouds.* Second edition, 671 pp., Oxford University Press, London, England.

McDonald, J. E. (1964), Cloud nucleation on insoluble particles, *J. Atmos. Sci.*, *21*(1), 109-116.

Möhler, O., C. Linke, H. Saathoff, M. Schnaiter, R. Wagner, A. Mangold, M. Krämer, and U. Schurath (2005), Ice nucleation on flame soot aerosol of different organic carbon content, *Meteorol. Z., 14*(4), 477–484.

Onasch, T. B., R. L. Siefert, S. D. Brooks, A. J. Prenni, B. Murray, M. A. Wilson, and M. A. Tolbert (1999), Infrared spectroscopic study of the deliquescence and efflorescence of ammonium sulfate aerosol as a function of temperature. *J. Geophys. Res., 104*(D17), 21317-21326.

Pant, A., M. T. Parsons, and A. K. Bertram (2006), Crystallization of aqueous ammonium sulfate particles internally mixed with soot and kaolinite: Crystallization relative humidities and nucleation rates, *J. Phys. Chem. A*, *110*(28), 8701–8709.

Pitter, R. L., and H. R. Pruppacher (1973), A wind tunnel investigation of freezing of small water drops falling at terminal velocity in air, *Q. J. R. Meteorol. Soc., 99*(421), 540– 550.

Pöschl, U. (2005), Atmospheric aerosols: composition, transformation, climate and health effects, *Angewandte Chemie International Edition*, *44*(46), 7520-7540.

Poulenard, J., J.C. Michel, F. Bartoli, J.M. Portal, P. Podwojewski (2004), Water repellency of volcanic ash soils from Ecuadorian páramo: effect of water content and characteristics of hydrophobic organic matter, *European J. Soil Sci.*, *55*(3), 487-496.

Prenni, A. J., M. E. Wise, *et al.* (2001) Ice nucleation in sulfuric acid and ammonium sulfate particles. *J. Geophys. Res., 106*(D3), 3037-3044.

Pruppacher, H. R., and J. D. Klett (1997), *The Microphysics of Clouds and Precipitation*, 2nd revised and enlarged edition, 954 pp., Kluwer Academic Publishers, Dordrecht, The Netherlands.

Rangno, A. L., and P. V. Hobbs (1990), Rapid development of ice particles concentrations in small polar maritime cumuliform clouds, *J. Atmos. Sci., 47*(22), 2710-2722.

Rangno, A. L., and P. V. Hobbs (1994), Ice particle concentrations and precipitation development in small continental cumuliform clouds. *Q. J. R. Meteorol. Soc., 120*(517), 573-601.

Roberts, P., and J. Hallett (1968), A laboratory study of the ice nucleating properties of some mineral particulates, *Q. J. R. Meteorol. Soc.*, *94*(399), 25-34.

Rogers, D. C. (1988), Development of a continuous flow thermal gradient diffusion chamber for ice nucleation studies. *Atmos. Res., 22*(22), 149-181.

Rogers, R. R. and M. K. Yau (1989), *A Short Course in Cloud Physics*, 3rd edition, 290 pp., Butterworth Heinemann, Oxford, UK.

Rosinski, J. and C.T. Nagamoto (1976), Contact nucleation of ice by natural aerosol particles, *J. Aerosol Sci*., *7*(1), 1-4.

Sax, R.I. and P. Goldsmith (1972), Nucleation of water drops by Brownian contact with AgI and other aerosols, *Q. J. R. Meteorol. Soc., 98*(415), 60–72.

Schnell, R. C., and G. Vali (1972), Atmospheric ice nuclei from decomposing vegetation, *Nature*, *236*(5343), 163-165.

Schnell, R. C. (1974), Biogenic sources of atmospheric ice nuclei, Ph.D. thesis, University of Wyoming, Laramie, WY.

Schnell, R. C., et al. (1982), Ice nucleus characteristics of Mount St. Helens effluents, *J. Geophys. Res., 87*(C13), 11109-11112.

Shaw, R. A., A. J. Durant, and Y. Mi (2005), Heterogeneous surface crystallization observed in undercooled water, *J. Phys. Chem. B*, *109*(20), 9865-9868.

Sigurbjörnsson, O.F., and R. Signorell (2008), Volume versus surface nucleation in freezing aerosols, *Phys. Review E*, *77*(5), 051601.

Sun, J., and P. A. Ariya (2006), Atmospheric organic and bio-aerosols as cloud condensation nuclei (CCN): A review, *Atmos. Environ.*, *40*(5), 795-820.

Tabazadeh, A., Y. S. Djikaev, and Reiss (2002), Surface crystallization of supercooled water in clouds*, Proc. Natl. Acad. Sci.*, *99*(25), 15873–15878.

Turnbull, D., and J. C. Fisher (1949), Rate of nucleation in condensed systems, *The J. Chemical Physics*, *17*(1), 71-73.

Vali, G. (1968), Ice nucleation relevant to formation of hail, Ph.D. thesis, McGill University, Montreal, Quebec, Canada.

Vali, G. (1971), Quantitative evaluation of experimental results and the heterogeneous freezing nucleation of supercooled liquids, *J. Atmos. Sci.*, *28*(3), 402-409.

Vali, G. (1985), Nucleation terminology*, J. Aerosol Sci*, *16*(6), 575–576.

Vali, G. (2008), Repeatability and randomness in heterogeneous freezing nucleation, *Atmospheric Chemistry and Physics Discussions, 8*(1), 4059-4097.

von Blohn, N., S.K. Mitra, K. Diehl, and S. Borrmann (2005), The ice nucleating ability of pollen: Part III: New laboratory studies in immersion and contact freezing

modes including more pollen types, *Atmos. Res*., *78*(3), 182–189.

Wallace, J. M., and P. V. Hobbs (2006), *Atmospheric Science: An Introductory Survey*, 2nd edition, 483 pp., Academic, San Diego, CA.

Wylie, D. P., W. P. Menzel, H. M. Woolf, and K. I. Strabala (1994), Four years of global cirrus cloud statistics using HIRS, *J. Climate*, *7*(12), 1972-1986.

Wyslouzil, B. E., K. L. Carleton, D. M. Sonnenfroh, and W. T. Rawlines (1994), Observation of hydration of single, modified carbon aerosols. *Geophys. Res. Lett., 21*(19), 2107-2110.

Yang, P., B. A. Baum, A. J. Heymsfield, Y. X. Hu, H.L. Huang, S.C. Tsay, and S. A. Ackerman (2003), Single-scattering properties of droxtals, *J. Quantitative Spectroscopy and Radiative Transfer*, *79*, 1159-1169.

Yao, Y., M. Massucci, S. L. Clegg, P. J. Brimblecombe (1999), Equilibrium water partial pressures and salt solubilities in aqueous NH_4HSO_4 to low temperatures. *J. Physical Chem. A, 103*(19), 3678-3686.

Young, K.C. (1974), The role of contact nucleation in ice phase initiation in clouds, *J. Atmos. Sci., 31*(3), 768–776.

Young, K. C. (1993), *Microphysical Processes in Clouds*, 427 pp., Oxford University Press, New York, NY.

APPENDIX A

The following appendix outlines the methodology behind a very simple optical technique used to verify the location of a nucleating particle implanted into a sessile water droplet on a horizontal surface. To determine the position of an implanted nucleating particle within a water droplet, we used a simple optical technique that exploited the distinct focal plane associated with compound light microscopes. This technique utilized a boom-mounted compound microscope set in a horizontal orientation. Such a configuration allowed the droplet to be viewed from the side, placing the focal plane perpendicular to the horizontal glass microscope slide on which the droplet resided. Thus by adjusting the focus on the microscope, it was possible to intersect the focal plane with the droplet as was previously depicted in Figure 2. Because of the well-defined focal plane offered by the microscope, quantitative measurements of particle position within a given droplet were possible. This was accomplished by orienting the droplet/particle system such that the particle was between and collinear with the center of the droplet and the objective lens, establishing a reference focal plane location within each droplet and then finally moving the focal plane until the particle was brought into focus.

The distance traversed by the objective lens during this process was measured by gradations on the microscope's fine focusing unit (to the nearest 0.001 mm) and used to determine the position of the particle relative to the reference focal plane within the droplet.

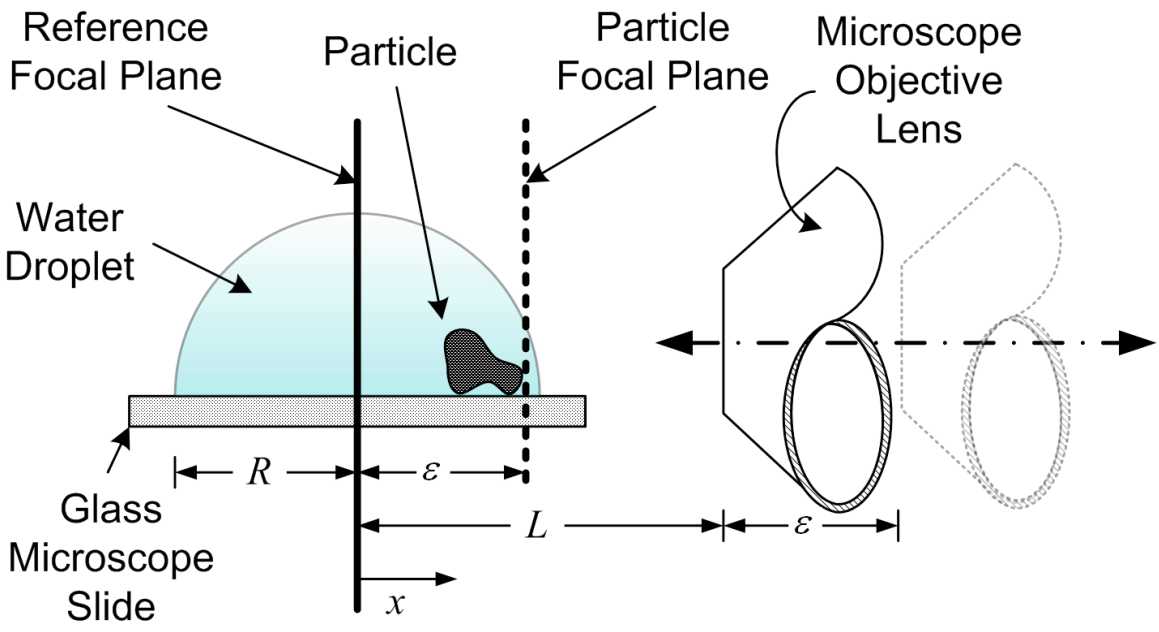

Figure 13: A slightly more complex illustration of our optical particle-locating method is shown here.

The overall concept associated with this approach is illustrated in Figure 13. Due to the semi-spherical shape of a given droplet of radius R, focusing on the center plane of the droplet at x = 0 proved to be the most reliable choice for the reference focal plane. And because the working distance of the objective lens, L, is constant, it follows that the distance traversed by the lens to bring the immersed particle into focus must be equal to the distance between the reference and particle focal planes given by ε. It should be noted that ε represents the distance from the reference focal plane to the edge of the particle closest to the outer edge of the droplet (or alternatively, the edge closest to the objective lens). Based on this methodology, we were able to verify whether or not a particle was partially or completely immersed in a given water droplet. Assuming that the droplet radius R is known a priori, a particle known to be much smaller than the droplet itself can

be considered fully immersed so long as $\varepsilon < |R|$.

VITA

Name:	Adam Patrick Fornea
Address:	Texas A&M Department of Atmospheric Sciences 1204 Eller O&M, 3150 TAMU College Station, TX 77843-3150
Email Address:	adam.fornea@gmail.com
Education:	B.S., Meteorology, Texas A&M University, 2006 M.S., Atmospheric Sciences, Texas A&M University, 2009